Applied and Environmental Microbiology

| Host-Microbial Interactions | Full-Length Text

Real-time genomic pathogen, resistance, and host range characterization from passive water sampling of wetland ecosystems

Albert Perlas,[1,2] Tim Reska,[1,2,3] Alberto Sánchez-Cano,[4] Cristina Mejías-Molina,[5,6] Daniel Gygax,[1,2,3,7] Sandra Martínez-Puchol,[5,6] Marta Rusiñol,[5,6] Elias Eger,[8] Katharina Schaufler,[8,9] Ursula Höfle,[4] Guillaume Croville,[10] Guillaume Le Loc'h,[10] Jean-Luc Guérin,[10] Lara Urban[1,2,3,11]

AUTHOR AFFILIATIONS See affiliation list on p. 18.

ABSTRACT Wetland ecosystems provide interfaces for the transmission of microbial pathogens and antimicrobial resistances (AMR) between migratory birds, wild and domestic animals, and human populations. The efficient surveillance of wetlands is, however, challenging, since the typically low concentration of pathogens requires the sampling of large volumes of water and subsequent targeted detection, which is inherently limited to a few pathogens or AMR genes of interest. Here, we present a holistic, accessible, and cost-efficient framework to characterize the pathogen and resistance load of water sources together with their potential associated hosts by combining passive water sampling through torpedo-shaped devices with nanopore sequencing technology. We used this framework to characterize anthropogenically influenced and natural wetland ecosystems along the East Atlantic Flyway, where we obtained robust assessments of the microbial communities from long-read metagenomic and RNA virome data and showed that anthropogenically impacted wetland ecosystems consistently exhibited higher relative abundances of pathogens and AMR genes. By focusing on avian influenza viruses (AIV), we finally highlight the additional need for targeted screening and whole-genome sequencing of pathogens of interest; we detected and characterized AIV at a third of the monitored sites and used environmental DNA to explore potential animal hosts to better understand the role of wetland ecosystems as One Health interfaces, where the health of animals, humans, and the environment are interconnected and pathogen transmission can occur across these domains.

IMPORTANCE Wetlands connect wildlife, livestock, and people, making them key places to watch for pathogens and antibiotic resistance. Yet potentially harmful microbes are easy to miss in water because they represent only a small fraction of the abundant microbial life in water, making them hard to detect. We paired 3D-printed passive torpedo-shaped samplers with a portable genetic sequencer to analyze all microbes captured. We deployed this approach at 12 wetlands in Germany, France, and Spain. It revealed local microbial communities, identified disease-causing bacteria, and linked many antibiotic resistance genes to likely bacterial hosts. By comparing locations, we observed that sites near cities, farms, or wastewater had higher levels of pathogens and resistance than protected natural sites. Our analysis also recovered all viruses present, including those from mammals, birds, fish, insects, and plants. We also specifically looked for the virus that causes avian flu, found it at several sites, and classified it as low pathogenicity. Because our method is non-invasive to wildlife, affordable, and practical to deploy, it can provide early warnings to conservation and public health agencies and guide action where risks are present.

Editor John R. Spear, Colorado School of Mines, Golden, Colorado, USA

Address correspondence to Albert Perlas, perlasalbert@gmail.com, Tim Reska, timreska@gmail.com, or Lara Urban, lara.h.urban@gmail.com.

Albert Perlas and Tim Reska contributed equally to this article. Albert Perlas additionally contributed to project funding acquisition and so is listed first.

The authors declare no conflict of interest.

See the funding table on p. 19.

Received 22 December 2025
Accepted 23 March 2026
Published 24 April 2026

KEYWORDS environmental pathogen surveillance, avian influenza, eDNA, nanopore sequencing, AMR, One Health, passive water sampling

Wetlands are among the most productive ecosystems on Earth, covering about 7% of the planet's surface while supporting an estimated 40% of global biodiversity (1). They provide critical ecosystem services such as climate regulation, flood control, carbon sequestration, and water purification, and they serve as essential habitats for migratory birds (2). Despite this importance, wetlands are under severe threat from anthropogenic pressures, with Europe alone having lost more than half of its wetland area since 1970 (3). Their degradation not only undermines biodiversity conservation but also poses significant risks for public health, exemplifying the interconnectedness of environmental, animal, and human health as captured by the One Health concept (4).

Pollutants introduced by agriculture and urbanization, such as nutrients, pesticides, heavy metals, and antimicrobials, reshape wetland microbial ecology and foster environmental reservoirs of pathogens and antimicrobial resistances (AMR) (5). AMR, now recognized by the World Health Organization as one of the top 10 global health threats (6), is driven in aquatic systems by the confluence of high microbial densities and sub-lethal antimicrobial concentrations, which facilitate horizontal gene transfer via mobile genetic elements (7). Among environmentally persistent pathogens of concern, *Vibrio cholerae* represents a notable example: while it is a naturally occurring aquatic bacterium, only toxigenic strains harboring the *ctxA* and *ctxB* genes cause cholera, underscoring the need for targeted virulence gene screening in environmental surveillance (8). Resistance genes that emerge in such environments can spread to clinically relevant pathogens and subsequently re-enter animal and human populations, underscoring the environment's role as a critical AMR reservoir (5).

In parallel, wetlands act as ecological interfaces for the maintenance and spread of zoonotic RNA viruses through migratory host networks. RNA viruses are of particular concern since they possess high evolutionary plasticity, enabling rapid host adaptation and establishing new transmission routes (9). RNA viruses also profit from global environmental changes, such as those caused by increased livestock density, global mobility, and deforestation (10), which further increases the risk of the emergence of new zoonotic pathogens. Various RNA viruses such as *Picornaviridae*, *Paramyxoviridae*, or *Orthomyxoviridae* (such as avian influenza viruses, or AIV) are known to infect waterfowl species that rely on wetlands as breeding, staging, and overwintering habitats and are therefore at risk of being globally distributed through migratory flyways (11). In the case of AIV, wild birds, particularly members of the order Anseriformes (e.g., ducks, geese, and swans), and Charadriiformes (e.g., gulls) often asymptomatically carry low pathogenicity AIV (LPAIV), leading to spillover events to poultry and subsequent evolution into high pathogenicity AIV (HPAIV) with devastating animal welfare, economic, and food security consequences (12). Since the emergence of the H5N1 "Gs/GD lineage" in 1996, it has additionally become clear that HPAIV can also be directly transmitted from wild birds to poultry (13). Along the East Atlantic Flyway, recurrent outbreaks of H5N1 HPAIV have contributed to the ongoing panzootic in Europe (14), with severe consequences not only for poultry production but also for wildlife conservation, as increasing numbers of wild bird species have proven susceptible to the current lineages (15, 16).

Traditional pathogen and AMR monitoring approaches from water ecosystems often rely on active filtration of large volumes of water (e.g., 10 L–50 L for AIV surface water surveillance and up to 500 L–1,000 L or more for diverse bacteria detection in drinking water systems), as in the case of AIV surveillance where the pathogen is expected to occur at low concentrations (17–19). Processing such large volumes is logistically challenging: field collection, preservation, and transport to the laboratory are difficult, and on-site filtration requires access to costly autosamplers and pumping equipment (18). Large-scale environmental surveillance, however, needs to be based on approaches that are inexpensive, simple to deploy and transport, and capable of integrating temporal and spatial signals. Recently developed 3D-printed, torpedo-shaped passive

samplers meet these requirements: the torpedo design helps the sampler stay clean and prevents waterborne debris buildup, allowing its deployment for extended timeframes (20). The samplers can be easily assembled with a standard 3D printer and deployed *in situ* at the point of care without specialized equipment or highly trained personnel. The torpedo-shaped passive sampler accommodates adsorptive media such as electronegative membranes to capture biological material during multi-day deployments (20). Originally optimized for wastewater surveillance of SARS-CoV-2, these devices have proven to be cost-effective, easy to install at scale, and sensitive to low pathogen concentrations, offering a practical alternative to grab sampling or autosampler-based approaches (20). Their simplicity and low cost have driven growing interest, and recent applications in urban wastewater have demonstrated effective surveillance not only of SARS-CoV-2, but also of fecal indicator bacteria and other respiratory viruses, including influenza A and B (20–24), as well as more recently AIV in wetland areas (25).

These studies have either relied on targeted approaches such as quantitative PCR detection or probe-based sequencing, which capture only a fraction of the microbial community, or on culture-based isolation (26), which can recover only a small proportion of the microbial diversity (27). To address these limitations, we combined torpedo-shaped passive water samplers with long-read genomics by nanopore sequencing. Nanopore sequencing technology allows for holistic pathogen and AMR monitoring by integrating DNA-based metagenomics with RNA virome characterizations (28–30). The long nanopore reads allow for the analysis of extended contiguous sequences, which makes taxonomic and functional inferences more robust (31), elucidates the genomic context of resistance genes (32, 33), and enables *de novo* assemblies for high-confidence pathogen and resistance gene detection (34–36). Whole RNA virome studies have revolutionized virus discovery and have advanced our understanding of natural viromes in both vertebrates and invertebrates; recently, a nanopore sequencing-based protocol further facilitates the assembly of viral taxa by integrating long-read technology (37–39). Due to its capability to also sequence short reads as generated in metabarcoding studies, nanopore sequencing technology can further be leveraged for vertebrate environmental DNA (eDNA) analysis (40, 41) to then identify potential wildlife or livestock hosts of the detected pathogens and resistances. We apply this framework to characterize the pathogen load, the presence of AMR, and the potential vertebrate host range from passive water sampling of wetland ecosystems along the East Atlantic Flyway, and to assess the potential implications of direct anthropogenic pressures on wetlands for public health.

MATERIALS AND METHODS

Wetland selection

We sampled 12 lentic wetland sites across Germany, France, and Spain, selected to represent anthropogenic and natural land-use categories (Table 1). Sites were coded using a [Country][Environment][Site Number] format, where Country is G (Germany), F (France), or S (Spain); and Environment is A (anthropogenic) or N (natural). The six anthropogenically impacted wetland sites were selected based on direct adjacency to known anthropogenic point sources: a landfill (GA1), urban areas (GA2–3), intensive duck farms (FA1–2), and a sewage treatment plant (SA1). These were compared with six proximal natural sites (at 5 km–15 km distance to the matched anthropogenic site), which lacked such direct anthropogenic inputs and included coastal marshes and peat bogs (GN1–3) and protected wetland reserves (FN1; SN1–2). This "natural" classification does not imply complete absence of anthropogenic pressures (such as, e.g., air pollution). None of the anthropogenic sites were designed for environmental mitigation purposes. All sites were characterized by standing or slow-moving water (lentic systems), minimizing flow-related variability in sampler performance and ensuring comparable sampling conditions across locations. Detailed site descriptions, GPS coordinates, and environmental parameters are provided in Table 1 and Fig. S1.

TABLE 1 Sampling data of all wetland sites, including site ID, sampling location (country and city), land use type, coordinates, and site description[a]

Site ID	Country	City	Land use type	Coordinates	Description
GA1	Germany	Greifswald	Anthropogenic	54.09950 N, 13.37606 E	Landfill runoff pond
GA2	Germany	Greifswald	Anthropogenic	54.10097 N, 13.34214 E	Village-edge wetland
GA3	Germany	Greifswald	Anthropogenic	54.09098 N, 13.36936 E	Urban pond
GN1	Germany	Greifswald	Natural	54.15939 N, 13.38237 E	Karrendorfer Wiesen meadow
GN2	Germany	Greifswald	Natural	54.15958 N, 13.38500 E	Coastal marsh adjacent to GN1
GN3	Germany	Greifswald	Natural	54.18415 N, 13.20164 E	Mannhagener Moor peat bog
FA1	France	Toulouse	Anthropogenic	43.57939 N, 0.94892 E	High-intensity duck farm pond
FA2	France	Toulouse	Anthropogenic	43.80843 N, 0.08469 E	High-intensity duck farm pond
FN1	France	Toulouse	Natural	43.76959 N, 1.33755 E	Wetland reserve
SA1	Spain	Ciudad Real	Anthropogenic	39.39584 N, –3.24058 W	Agricultural drainage wetland near a landfill
SN1	Spain	Ciudad Real	Natural	39.07572 N, –3.91176 W	Peralbillo reserve
SN2	Spain	Ciudad Real	Natural	39.14011 N, –3.69563 W	Marsh at the edge of Las Tablas de Daimiel National Park

[a]An interactive Google Earth map can be found here: https://www.bit.ly/locations_pathogen.

Passive water sampling

Passive water sampling was conducted using 3D-printed torpedo-shaped passive sampler units developed by the McCarthy group (Queensland University of Technology, Australia) (20). These torpedoes are designed to reduce clogging and fouling during deployment and can accommodate various passive sampling materials. For this study, each unit contained two 0.45 µm mixed cellulose ester electronegative membranes (Whatman, Merck) for microbial particle adsorption. Two or three passive samplers were deployed at each wetland site. Each sampler was attached to a metal rod driven into the sediment using cable ties, positioning them 20 cm below the water surface to ensure continuous submersion while avoiding sediment contact. After 3 days in the water column, samplers were retrieved, visually inspected to remove debris, dismantled, and the membranes were transferred to bead-beating tubes for subsequent nucleic acid extraction.

Dual DNA and RNA extraction

From the bead-beating tubes with the electronegative membranes, we performed simultaneous extraction of DNA and RNA using the AllPrep PowerFecal Pro DNA/RNA kit (QIAGEN, 2018, Hilden, Germany), following the manufacturer's protocol with modified elution volumes (25 µL DNA, 50 µL RNA). DNA and RNA yields were quantified using Qubit 4.0 High Sensitivity assays (Invitrogen, 2021). Negative controls included field blanks, extraction blanks, and sequencing blanks, which were processed identically to the environmental samples.

Nanopore sequencing

Four parallel real-time genomic sequencing by nanopore sequencing approaches were employed: from DNA, we performed (i) shotgun metagenomics to characterize microbial communities and detect antimicrobial resistance genes and (ii) 12S rRNA metabarcoding for vertebrate species detection; from RNA, we performed (iii) RNA virome analysis and (iv) targeted detection of AIV by qPCR followed by whole-genome viral sequencing. Nanopore sequencing was performed on portable Oxford Nanopore Technologies (Oxford, UK) MinION Mk1c or Mk1d sequencers using R10.4.1 flow cells. Sequencing runs were conducted for 24 h using the MinKNOW v.24.11.10 software, with data acquisition at 5 kHz, a minimum quality score of 9, and a minimum read length threshold of 20 bases.

Shotgun metagenomics

Nanopore sequencing libraries from 24 samples (12 sites × 2 replicates) were generated using the Rapid Barcoding Kit (SQK-RBK114.24). To balance sequencing yield across samples, each sample was assigned two unique barcodes per sequencing run, with data from both barcodes combined during downstream analysis. To achieve equimolar pooling, samples were divided into two batches based on DNA concentration: eight high-concentration samples were pooled and distributed across two flow cells, and 16 lower-concentration samples plus sequencing blanks were pooled separately and distributed across another two flow cells, following established protocols (35). One negative sequencing control was included per flow cell. One sampling and two extraction negative controls were sequenced separately.

Vertebrate metabarcoding

We PCR-amplified a ~97 base pair (bp) fragment of the mitochondrial 12S rRNA gene (V5 region) from the eDNA extracts from our 12 locations, one technical negative control, one negative control of extraction, and one positive control following our previously established protocol (41). Briefly, we used the broad-vertebrate primer set 12SV05 (forward 5′-TTAGATACCCCACTATGC-3′, reverse 5′-TAGAACAGGCTCCTCTAG-3′) developed by Riaz et al. (42). Unique 9 bp tags (with ≥3 bp differences between any two tags) were appended to both primers for sample multiplexing. The PCR mix (20 µL volume) contained 3 µL of template DNA, 0.75 U AmpliTaq Gold polymerase, 1× Gold Buffer, 2.5 mM $MgCl_2$, 0.2 mM each dNTP, 0.6 µM of each tagged primer, and 0.5 mg/mL bovine serum albumin. To suppress human DNA amplification, a 3 µM human-blocking oligonucleotide (5′-TACCCCACTATGCTTAGCCCTAAACCTCAACAGTTAAATC-3′, with a 3′ C3 spacer) was included in each reaction, following reference 43. The PCR thermal profile was initial denaturation at 95°C for 10 min; 45 cycles of 94°C for 30 s, 60°C for 30 s, 70°C for 60 s; and a final extension at 72°C for 7 min. Successful amplification was confirmed on 2% agarose E-Gel gels (Thermo Fisher). Amplicon pools from each sample were then combined (18 µL per PCR), purified with HigherPurity magnetic beads (1:1 ratio), and eluted in 50 µL of DNA-free water. One sequencing library was prepared from the purified 12S rRNA amplicon pool using the Ligation Sequencing Kit (SQK-LSK114) in one flow cell.

RNA virome

RNA extracts were processed following the Rapid SMART-9N protocol described by reference 29, which uses random priming and a template-switching mechanism to generate long-length complementary DNA (cDNA) flanked by known sequences for downstream PCR barcoding. Briefly, residual DNA was removed from 44 µL RNA by treatment with 5 µL TURBO DNase buffer and 1 µL TURBO DNase (Thermo Fisher Scientific) at 37°C for 30 min. RNA was then purified and concentrated to 10 µL using the RNA Clean & Concentrator-5 kit (Zymo Research). For first-strand cDNA synthesis, 10 µL RNA was mixed with 1 µL RLB RT 9N primer (5′-TTTTTCGTGCGCCGCTTCAAC NNNNNNNNN-3′, 2 µM), a random-priming oligonucleotide with a fixed 5′ sequence complementary to the PCR primers, and 1 µL of 10 mM dNTPs, incubated at 65°C for 5 min, and placed on ice. Eight microliters of this mixture were reverse transcribed in a 20 µL reaction containing the annealed RNA, 4 µL SuperScript IV First-Strand Buffer, 1 µL 0.1 M DTT, 1 µL RNaseOUT, 1 µL RLB TSO oligo (5′-GCTAATCATTGCTTTTTCGTGCGCC GCTTCAACATrGrGrG-3′, 2 µM), which hybridizes to non-templated cytosines added by the reverse transcriptase and adds a second fixed sequence at the cDNA 5′ end, and 1 µL SuperScript IV reverse transcriptase (Thermo Fisher Scientific). The reaction was incubated at 42°C for 90 min followed by 70°C for 10 min. The resulting double-tagged cDNA was amplified in a 50 µL PCR reaction containing 5 µL cDNA, 25 µL LongAmp Taq 2× Master Mix (New England Biolabs), 19.5 µL nuclease-free water, and 0.5 µL RLB barcode primer (SQK-RPB114.24), which binds the fixed primer sites at both cDNA ends

and incorporates a sample-specific barcode. PCR cycling conditions were: 95°C for 45 s; 25–30 cycles of 95°C for 15 s, 56°C for 15 s, and 65°C for 5 min; final extension at 65°C for 10 min. Amplicons were purified using a 1:1 AMPure XP bead ratio (Beckman Coulter) and quantified with a Qubit 4.0 fluorometer using the dsDNA High Sensitivity Assay Kit (Thermo Fisher Scientific). Sequencing libraries were prepared with the Rapid Sequencing PCR Barcoding Kit (SQK-RPB114.24) and sequenced on two flow cells.

AIV analysis

AIV detection was performed by applying reverse transcription (RT)-qPCR to the extracted RNA while targeting a highly conserved region of the influenza matrix 1 (M1) gene with a one-step TaqMan RT-PCR in a Fast7500 equipment (Applied Biosystems), using primers (M+ 25 5′-AGATGAGTCTTCTAACCGAGGTCG-3′, M-124 5′-TGCAAAAACATCT TCAAGTCTCTG-3′) and probe (M+ 64 FAM 5′-TCAGGCCCCCTCAAAGCCGA-3′TAMRA) (44), and adding bovine serum albumin to increase sensitivity and avoid PCR inhibitors (45). Whole-genome AIV sequencing of positive samples was performed after complementary DNA (cDNA) conversion and multi-segment amplification using M-RTPCR (46), targeting conserved regions across all AIV segments: Briefly, the RNA was mixed with SuperScript III One-Step PCR (Invitrogen) buffer and enzyme mix (containing the reverse transcriptase enzyme and the PCR amplification enzyme). The thermal cycle parameters were 42°C for 60 min, 94°C for 2 min, and then 5 cycles (94°C for 30 s, 45°C for 30 s, and 68°C for 3 min), followed by 31 cycles (94°C for 30 s, 57°C for 30 s, and 68°C for 3 min). Primers used were MBTuni-12 (5′-ACGCGTGATCAGCAAAAGCAGG) and MBTuni-13 (5′-ACGCGTGATCAGTAGA AACAAGG) that correspond to the 5′ and 3′ conserved sequences of all eight influenza A segments, and that have been demonstrated effective on all subtypes. We finally used the Rapid Barcoding Kit (SQK-RBK114.24) (46) and sequenced the library on one flow cell.

Bioinformatic analysis

Nanopore data processing

Raw nanopore signal data (POD5) from all sequencing runs were basecalled using Dorado v5.0.0 in super-accuracy mode (dna_r10.4.1_e8.2_400bps_sup@v5.0.0; [47]). Demultiplexing and adapter/barcode trimming for shotgun and virome reads were performed with Porechop (v0.2.4) (48). Reads shorter than 100 bases (150 bases for AIV sequencing analysis) and reads with quality score below 9 (quality score below 8 for AIV sequencing analysis) were discarded using NanoFilt (v2.8.0) (49).

Metagenomic taxonomic classification

Quality-filtered nanopore reads were taxonomically classified using Kraken2 v2.1.2 (50) against the NCBI nt_core database (May 2025). For community composition analyses, all water samples were downsampled to 87,000 reads using SeqKit v2.3.0 (51). Sample GA3.1 (28,000 reads) was excluded due to insufficient sequencing depth. β-Diversity between samples was quantified using Bray-Curtis dissimilarity on genus-level reads and visualized by principal coordinate analysis (PCoA). No filtering was applied prior to β-diversity analysis; all detected genera were retained for Bray-Curtis dissimilarity calculation and PCoA. For visualization, the 20 most abundant microbial genera at a minimum relative abundance of 1% were visualized with stacked bar plots generated in Python (v3.12) using the pandas and matplotlib libraries. Genera with relative abundance below 1% were grouped into the "Others" category.

De novo assembly was performed using metaFlye (v2.9.6) (52) and nanoMDBG (v1.1) (53) to identify the optimal approach for our data set. The metaFlye assemblies underwent a polishing workflow: reads were first realigned to the assemblies using minimap2 (v2.28) (54), followed by three iterative rounds of polishing with Racon (v1.5.0) (55) and Medaka (v1.7.2) (56). NanoMDBG assemblies were polished with Medaka (v1.7.2)

alone. Assembled contigs were subsequently annotated using Kraken2 for taxonomic classification and Prokka v1.14.5 for functional annotation (57).

Metagenomic pathogen and virulence analyses

For stringent pathogen identification, reads and contigs were aligned to the NCBI nt_core databases using minimap2 (v2.28) and processed with MEGAN-CE v6.21.1 (58), using the lowest common ancestor assignment. Taxonomic assignment was only accepted if more than 50% of near-best alignments for a read matched the same genus. This conservative approach, combined with a strict LCA threshold, ensures high-confidence species-level assignments by classifying ambiguously mapped sequences at higher taxonomic ranks. Pathogenic species were subsequently identified using the Chan Zuckerberg ID initiative pathogen species list (CZ ID Pathogen list v0.2.1; 05/06/2024) (59). Only pathogenic species with at least five reads in a given replicate (or sampling site) were considered for downstream analysis.

To further investigate the pathogenic potential of *Vibrio cholerae*, targeted screening for specific virulence factors was conducted: alignments against the core protein data set of the Virulence Factor Database (60) were performed using DIAMOND BLASTx (v2.1.13) (61) to specifically search for reads corresponding to the cholera toxin subunit genes, *ctxA* and *ctxB* (60).

AMR and virulence genes were detected using AMRFinderPlus v4.0.23 (62) in --plus mode on the complete data set with its default thresholds (including minimum sequence identity of 90%). For assembled contigs, open reading frames were predicted with Prodigal v2.6.3 (63), enabling nucleotide- and protein-level analyses with AMRFinderPlus to maximize sensitivity. Pathogen-AMR associations were considered high-confidence when the same resistance gene was detected on both reads and contigs from a sample, and when the same reads/contigs were taxonomically linked to the same pathogen.

To assess the mobility potential of detected AMR genes, assembled contigs were screened for plasmids using PlasmidFinder v2.1.6 (64) against the PlasmidFinder database.

Avian host detection from eDNA

Basecalled 12S rRNA amplicon reads were demultiplexed by their 9 bp primer tags using OBITools4 obimultiplex (version 1.3.1) (65), allowing up to two mismatches in tag recognition. Primer sequences were trimmed from reads with Cutadapt (v4.2) (66). The reads were then processed in VSEARCH (v.2.21) (67): we filtered reads by expected error (maxEE 1.0) to remove low-quality reads, dereplicated reads (discarding singletons), removed chimeras, and clustered the remaining sequences into operational taxonomic units (OTUs) at 97% similarity. Each OTU representative sequence was taxonomically identified by global alignment against the MIDORI2 reference database of mitochondrial sequences (version "Unique 266") (68). Assignments were limited to bird species (Aves class) and accepted as robust if an alignment covered ≥80% of the query, had ≥98% identity, and if a taxonomic assignment had at least five reads as hits after OTU aggregation of same-species detection. When species-level calls were biogeographically implausible for our sampling sites (i.e., the species is not present in the sampled area), we collapsed the assignment to a higher rank (i.e., genus or family) or removed the record if no meaningful higher-rank assignment was possible. Regional occurrence (presence/absence) was assessed with eBird (https://ebird.org/home). Multiple OTUs mapping to the same retained taxon within a sample were summed to produce per-taxon read counts.

RNA virome taxonomic analysis

De novo assembly was performed using nanoMDBG (v1.1) and polished with Medaka (v1.7.2). Assembled contigs were compared against the NCBI non-redundant protein

database (NR database, accessed May 2025) using DIAMOND BLASTx (v2.1.13) (61). Contigs with a percentage identity above 80% when matched to the kingdom "Viruses" (NCBI taxid: 10239) were annotated as viral contigs.

AIV whole-genome sequencing analysis

The whole-genome AIV sequencing FASTQ files were aligned to the reference genomes using minimap2 (v2.28) (54) with the -ax map-ont setting. We used a reference database generated for each segment from the NCBI Influenza Virus Database, which contains all AIV nucleotide sequences from Europe (as of 04/03/2023). The resulting SAM files were converted to BAM format, sorted, and indexed using SAMtools (v1.17) (69). Using samtools idxstats, we selected the segment reference to which most reads mapped across every segment. All our reads were then mapped to the best reference for each of the eight segments of the influenza genome using minimap2 (v2.28), and genome coverage distributions were obtained. We then obtained the final AIV consensus sequence with BCFtools (v1.17) (70). For subtyping of H4 hemagglutinin (HA) consensus segment, we used the GISAID BLAST tool (71) and FluSurver (http://flusurver.bii.a-star.edu.sg).

To contextualize the H4 HA consensus sequence, we downloaded all publicly available full-length H4 HA sequences from GISAID since 2015 (accessed on 25 August 2025). Metadata (host, location, and collection date) were curated from the associated GISAID isolate tables. To reduce redundancy and improve tree readability, we implemented a stratified subsampling approach: sequences were grouped by host, country, and year, and up to three representatives per group were retained randomly. Multiple sequence alignment was performed with MAFFT (v7.526) (72). The aligned data set was used to infer a maximum-likelihood phylogeny with IQ-TREE2 (v2.3.4) (73) under the best-fit nucleotide substitution model selected by ModelFinder Plus (-m MFP). Node support was assessed with 1,000 ultrafast bootstrap replicates (-bb 1,000) and 1,000 SH-aLRT replicates (-alrt 1,000). The resulting tree was visualized in iTOL (v7) (74).

RESULTS

Nanopore sequencing data

After dual-nucleotide extraction of the electronegative membranes from the torpedo-shaped passive samplers (Materials and Methods), DNA yields ranged from below detection limit to 918 ng (Table S1), while RNA yields ranged from below detection to 3,335 ng (Table S2; Fig. S2A). Metagenomic sequencing generated 28k to 863k reads after filtering (median lengths 485–1,534 bp). 12S rRNA amplicon sequencing generated 19M reads after filtering. RNA virome sequencing produced 87k to 2.1M reads (median lengths 375–1,663 bp; Table S2; Fig. S2B through E). AIV sequencing generated 600k reads after filtering (median length 323).

Microbial taxonomic compositions across wetland sites

Taxonomic classification success varied considerably, with 13k–365k (corresponding to 16%–54%) metagenomic reads assignable to microbial genus level. After downsampling to 87k reads for comparative analysis, one sample (GA3.1) was excluded due to insufficient reads (Fig. S2F). All negative controls resulted in low DNA yields (<0.1 ng). Sampling negative controls included read mapping to the *Homo*, *Sphingomonas*, and *Timema* genera. Extraction negative controls included reads mapping to *Homo*, *Mus*, and *Timema* genera. Sequencing negative controls included reads mapping to the *Homo*, *Timema*, *Photobacterium*, and *Rheinheimera* genera. All pathogen-containing genera were absent from all negative controls (Table S1).

The microbial communities at the taxonomic genus level per site were highly similar in the respective biological replicates but otherwise did not show any clustering according to land usage or country of origin (Fig. 1A). Within the German sites, anthropogenic samples exhibited higher relative abundances of *Paracoccus* and *Pseudomonas*,

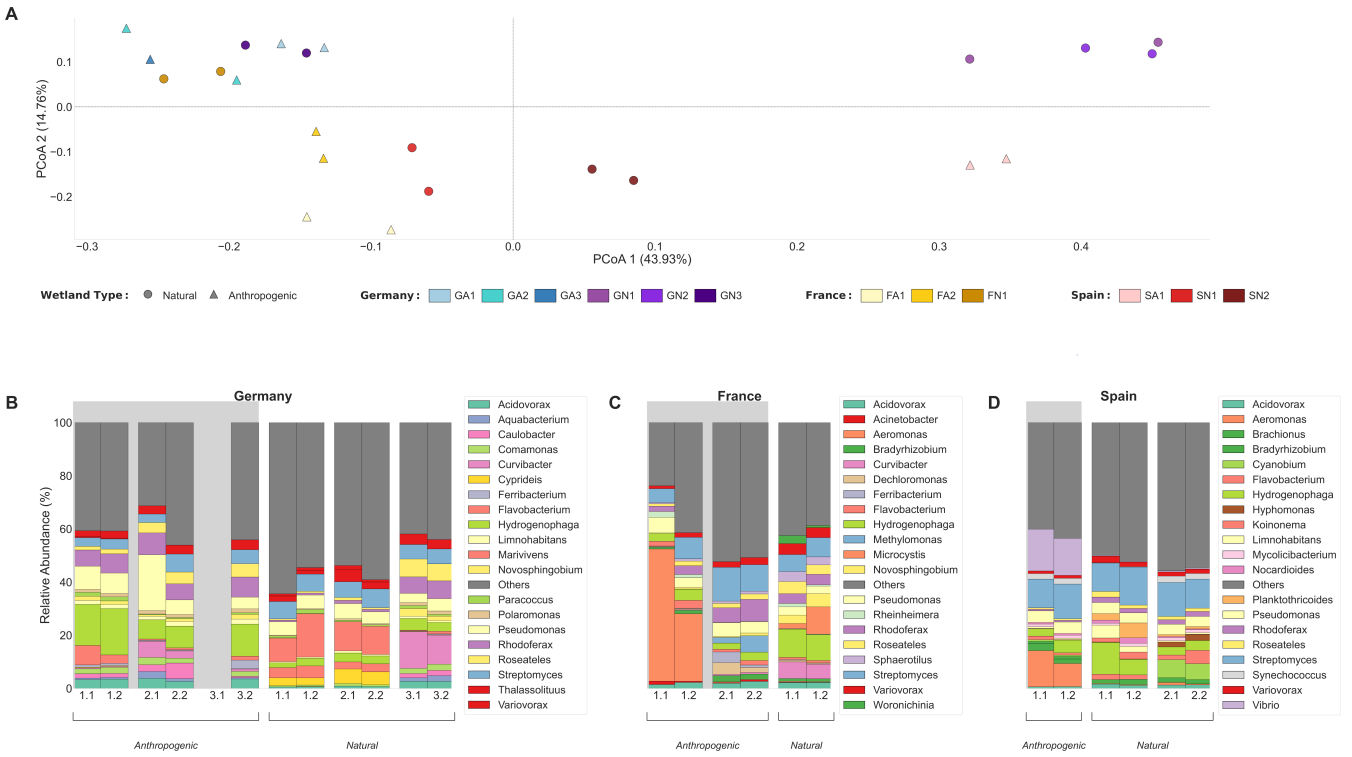

FIG 1 Microbial taxonomic composition at the genus level across wetland sites (after downsampling; two biological replicates per sample; see Materials and Methods). (A) Principal coordinate analysis (PCoA) of Bray-Curtis dissimilarities. Sites were coded using a [Country][Environment][Site Number] format, where Country is G (Germany; blue-purple gradient), F (France; yellow gradient), or S (Spain; red gradient); and Environment is A (anthropogenic; triangular shape) or N (natural; circular shape). (B–D) Relative abundance of the 20 most abundant bacterial genera for (B) Germany (including one replicate dropout after downsampling), (C) France, and (D) Spain. The *x*-axis shows site codes corresponding to Table 1. Gray background shading indicates anthropogenically impacted sites, while white background indicates natural wetlands. Genera below 1% relative abundance are grouped as "Others" (dark gray) for visualization purposes.

whereas natural sites showed increased *Marivivens* and *Curvibacter* (Fig. 1B). French sites displayed distinct, site-specific profiles: FA1 was dominated by *Aeromonas*, FA2 by *Streptomyces*, and FN1 by *Hydrogenophaga* (Fig. 1C). The Spanish anthropogenic site SA1 was enriched for *Vibrio* and *Aeromonas*, while natural sites showed higher *Streptomyces* and freshwater-associated taxa, including phototrophs such as *Cyanobium* and *Limnohabitans* (Fig. 1D).

Microbial pathogen and antimicrobial resistance detection across wetland sites

Anthropogenically impacted wetland sites contained a >13-fold higher number of pathogen-associated reads (9,346 reads across 17 unique species) compared to natural wetlands (703 reads across 15 unique species). Stringent microbial pathogen species assignment confirmed the presence of pathogens at all sites (Table S3; Materials and Methods). The French duck farm (FA1) showed the highest pathogen diversity and relative abundance, with the presence of several pathogenic *Aeromonas* species: *A. veronii* (2,960 and 656 reads in FA1.1 and FA1.2), *A. hydrophila* (223 and 481 reads), *A. caviae* (81 and 45 reads), and also *Pseudomonas putida* (212 and 189 reads) (Fig. 2). The Spanish anthropogenic site (SA1) had 1,809 reads mapping to *Vibrio cholerae*, with co-detection of *A. veronii* (139 reads) (Fig. 2).

Resistome analysis on the sequencing read level led to the detection of several AMR genes in both biological replicates taken from the anthropogenically impacted French (FA1) and Spanish (SA1) wetland sites (Table 1; Materials and Methods). The French wetland FA1, which was adjacent to a duck farm, contained nine distinct

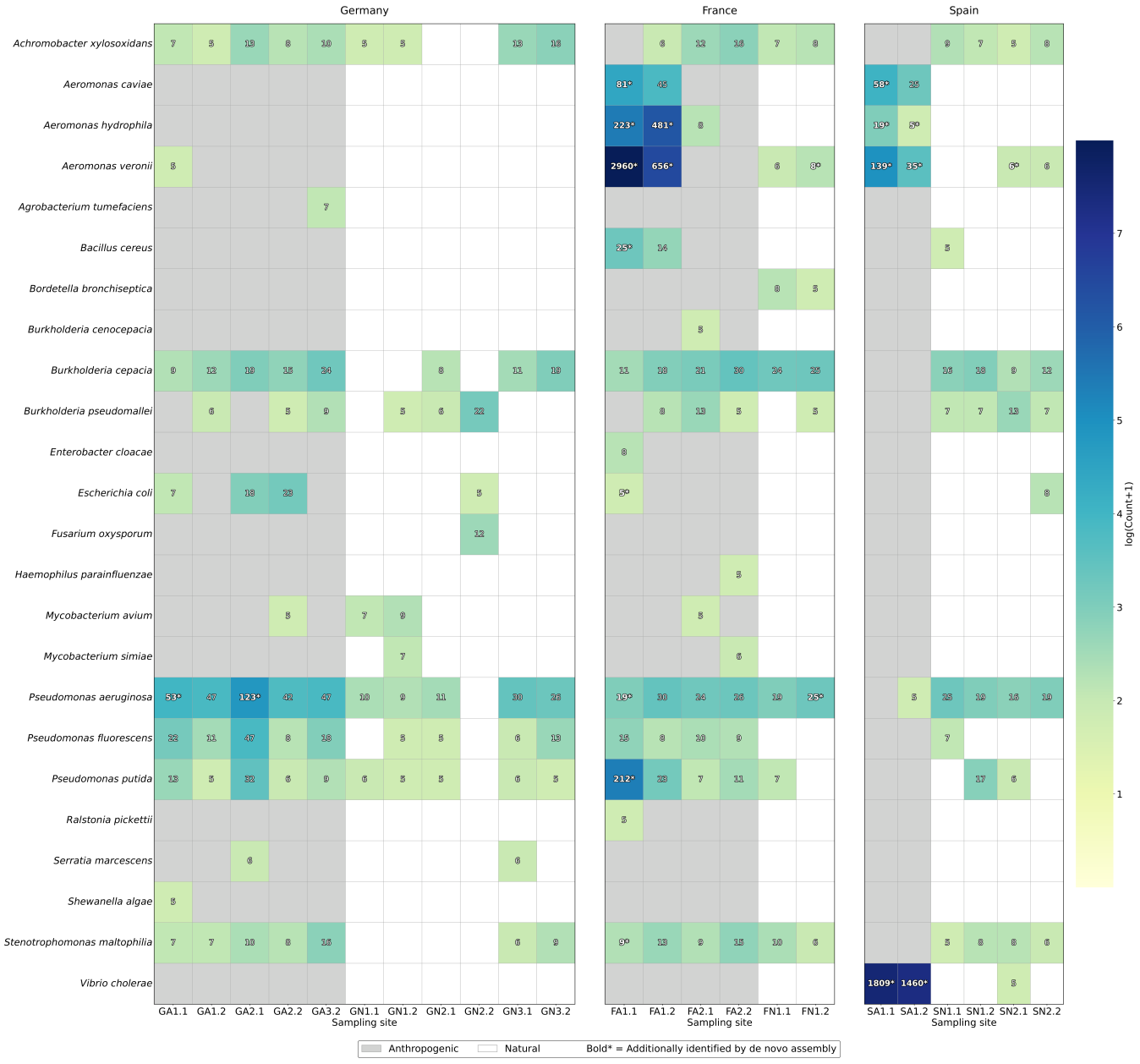

FIG 2 Number of sequencing reads assigned to pathogenic bacterial species across wetland sites (after downsampling; two biological replicates per sample; see Materials and Methods). The gray background highlights anthropogenically impacted sites. The reads assigned to pathogenic species that were additionally identified by *de novo* assemblies are highlighted in bold.

AMR genes, dominated by β-lactamases conferring resistance to β-lactam antibiotics: bla_{OXA} (extended-spectrum β-lactamase), *cphA* and *cphA1* (metallo-β-lactamases conferring carbapenem resistance), and bla_{FOX} (AmpC-type cephalosporinase). The Spanish wetland SA1 harbored 12 unique AMR genes, including bla_{VCC-1}, an Ambler class A carbapenemase. Sulfonamide resistance genes (*sul1*, *sul2*), which confer resistance to sulfonamide antibiotics commonly used in agriculture, were detected at both FA1 and SA1. While the GN3.2 sample contained one AMR gene, the bla_{CAU} gene, we excluded this sample from subsequent AMR analyses since this gene has been described as an intrinsic gene in environmental *Caulobacter crescentus* (75).

We used the taxonomic assignment of AMR gene-containing sequencing reads to link AMR genes to pathogenic microbial species (Table 2). At FA1, we found that the

TABLE 2 Number of detected antimicrobial resistance (AMR) genes across AMR-positive wetland sites[a]

Gene	FA1.1	FA1.2	SA1.1	SA1.2
aac(3)-I	0	2*	0	0
aadA1	0	0	2	4
almE	0	0	0	2*
almF	0	0	1*	3**
almG	0	0	2*	3*
bla_{FOX}	**3**	3*	0	0
bla_{OXA}	**68***	10*	1	0
$bla_{OXA-956}$	**4***	0	0	0
bla_{VCC}	0	0	5**	5**
bla_{VCC-1}	0	0	1**	1
catB2	0	0	4	2
cphA	**47***	0	**2****	0
cphA1	6**	1	2**	2
dfrA	0	0	2	1
dfrA1	0	0	2	2
emhA	**2**	0	0	0
mexE	5	0	0	0
sul1	0	0	3	4
sul2	1	2	0	0

[a]AMR detection was done on the sequencing read-level using AMRFinderPlus; all genes that had at maximum one hit across all samples were excluded. A single asterisk (*) indicates AMR gene counts that could be assigned to pathogenic bacterial species; a double asterisk (**) indicates AMR gene counts that could be assigned to a bacterial genus that is likely pathogenic; bold AMR gene counts were confirmed by detection on *de novo* assemblies of pathogenic bacterial species in the same sample (Materials and Methods). The GN3.2 sample is excluded since it only contains bla_{CAU} as an intrinsic gene in environmental *Caulobacter crescentus*.

$bla_{OXA-956}$, bla_{OXA}, and *cphA* genes were encoded by the pathogen *Aeromonas veronii*. To further assess the pathogenic potential of taxa carrying AMR genes beyond our stringent pathogenic species annotation criteria, we expanded our analysis to the genus level in cases where the detected genus was predominantly pathogenic in the same sample (Materials and Methods). At SA1, bla_{VCC} and bla_{VCC-1}-carrying reads were assigned to the *Vibrio* genus, and most Vibrio-assigned reads in the same sample could be classified as the pathogenic *Vibrio cholerae*. Similarly, *cphA*- and *cphA1*-carrying reads were assigned to the *Aeromonas* genus, and most reads in the same sample could be classified as the pathogenic *A. veronii*, *A. hydrophila*, and *A. caviae* species (Table 2).

To validate pathogen detections and pathogen-AMR associations at increased confidence, we repeated our analyses at the *de novo* assembly level (see bold numbers in Fig. 2; Table 2). While metaFlye generated assemblies with superior contiguity metrics, nanoMDBG yielded greater total assembly size, contig count, taxonomic diversity, and gene content (Fig. S2; Table S1; Materials and Methods). Based on nanoMDBG assemblies, anthropogenic and natural sites yielded 892 and 5 contigs assigned to pathogenic species, respectively. At FA1, 191 contigs were assigned to *Aeromonas veronii* (Table S4), with multiple contigs carrying β-lactamase genes previously identified in the read analysis: three contigs harbored *cphA* metallo-β-lactamase genes, three carried bla_{OXA} genes, and one contained the $bla_{OXA-956}$ variant (Table 3). Additionally, two contigs that were assigned to *Escherichia coli* contained the bla_{FOX} β-lactamase (Table 3). At SA1, 235 contigs mapped to *Vibrio cholerae*, and these contigs lacked the typical cholera toxin genes *ctxA* and *ctxB* (Table S4; Materials and Methods). The *de novo* assemblies additionally revealed previously undetected AMR genes. At FA1, contigs classified as *Acidiphilium multivorum* harbored arsenic resistance genes *arsB* and *arsC*, and one contig classified as *Acinetobacter pittii* harbored the nickel-resistance gene *nreB* (Table 3). No plasmids were detected in any sample.

TABLE 3 Resistance gene detection on the assembly level[a]

Location	Sample_ID	Gene	No. of contigs	Mean contig length (bp)	Taxonomy
FA1	FA1.1	*arsB*	1	6,726	*Acidiphilium multivorum*
FA1	FA1.1	*arsC*	4	1,159,374	*Acidiphilium multivorum*
FA1	FA1.1	bla_{FOX}	2	140,273	*Escherichia coli*
FA1	FA1.1	bla_{OXA}	3	1,529,006	*Aeromonas veronii*
FA1	FA1.1	$bla_{OXA-956}$	1	18,038	*Aeromonas veronii*
FA1	FA1.1	*cphA*	3	1,517,336	*Aeromonas veronii*
FA1	FA1.1	*emhA*	1	268,160	*Pseudomonas protegens*
FA1	FA1.1	*nreB*	1	14,017	*Acinetobacter pittii*
FA1	FA1.2	$bla_{OXA-956}$	1	545,020	*Aeromonas veronii*
SA1	SA1.1	*aac(6')*	1	1,285	*Pseudomonas aeruginosa*
SA1	SA1.2	*cphA*	1	17,170	*Aeromonas veronii*

[a]For each antimicrobial and resistance gene, the wetland site, the biological replicate, the number of assembled contigs, the mean length of those contigs in base pairs (bp), and the taxonomic assignment of those contigs are indicated.

eDNA-based avian host inference

We detected avian eDNA using 12S rRNA metabarcoding at most of the wetland sites, except for GN1–3 and GA2 (Fig. 3; Materials and Methods). Overall, detections were dominated by common waterfowl birds, with dabbling ducks (*Anas*, *Spatula*, and *Mareca*), geese (*Anser*), swans (*Cygnus*), and cormorants (*Phalacrocorax*) being the most common taxa (Fig. 3). The species richness (species per location) was highest at SN1 and FA1, followed by FA2 and SA1 (Fig. 3). No avian taxa were detected in any negative control.

RNA virome analysis

The percentage of sequencing reads assigned to the viral kingdom after random amplification of extracted RNA ranged from 0.1% to 1.26% (Table S2; Materials and Methods). After *de novo* assembly (Materials and Methods), the contigs assigned to the viral kingdom ranged from none (FA1, FA2, and SA1) to 4.54% at GA3 (Table S2). Due to unspecific taxonomic classification at the species and genus level, we focused our viral taxonomic classification on the family level. We overall found 93 contigs assigned to viral families, ranging from 0 contigs to 29 contigs per site (Table S2), and covering 13 distinct viral families (Fig. 4). The *Dicistroviridae* (20 contigs) and *Fiersviridae* (19 contigs) viral families were the most common ones (Fig. 4). The *Picornaviridae* viral family, which is the only one that contains several potential mammalian and bird pathogens, was only detected in a few contigs (Fig. 4). Viral contig recovery was highest at GA3 (29 contigs), followed by GN2 (17 contigs; Fig. 4).

AIV detection and sequencing

We detected AIV from passive samplers at four of the 12 sampled wetland locations (Table 4), including all three wetland sites in France, which were located in the vicinity of duck farms, and one wetland site in Spain, which was located close to a national park. The qPCR cycle threshold (Ct) values of the positive samples ranged from 34 to 40, with 40 representing the limit of detection (Table 4). HA subtyping by multi-segment PCR and whole-genome sequencing was successful only for one sample from site FA2. The HA consensus sequence had an average coverage depth of 160× and was classified as subtype H4, corresponding to a low pathogenicity AIV (LPAIV). We built a phylogenetic tree to place this strain in the evolutionary context of H4 viruses detected in Europe over the past 10 years (Fig. S4).

To identify potential avian hosts associated with AIV-positive wetlands, we overlapped our vertebrate eDNA-based species detections (Fig. 3) with official reports of AIV

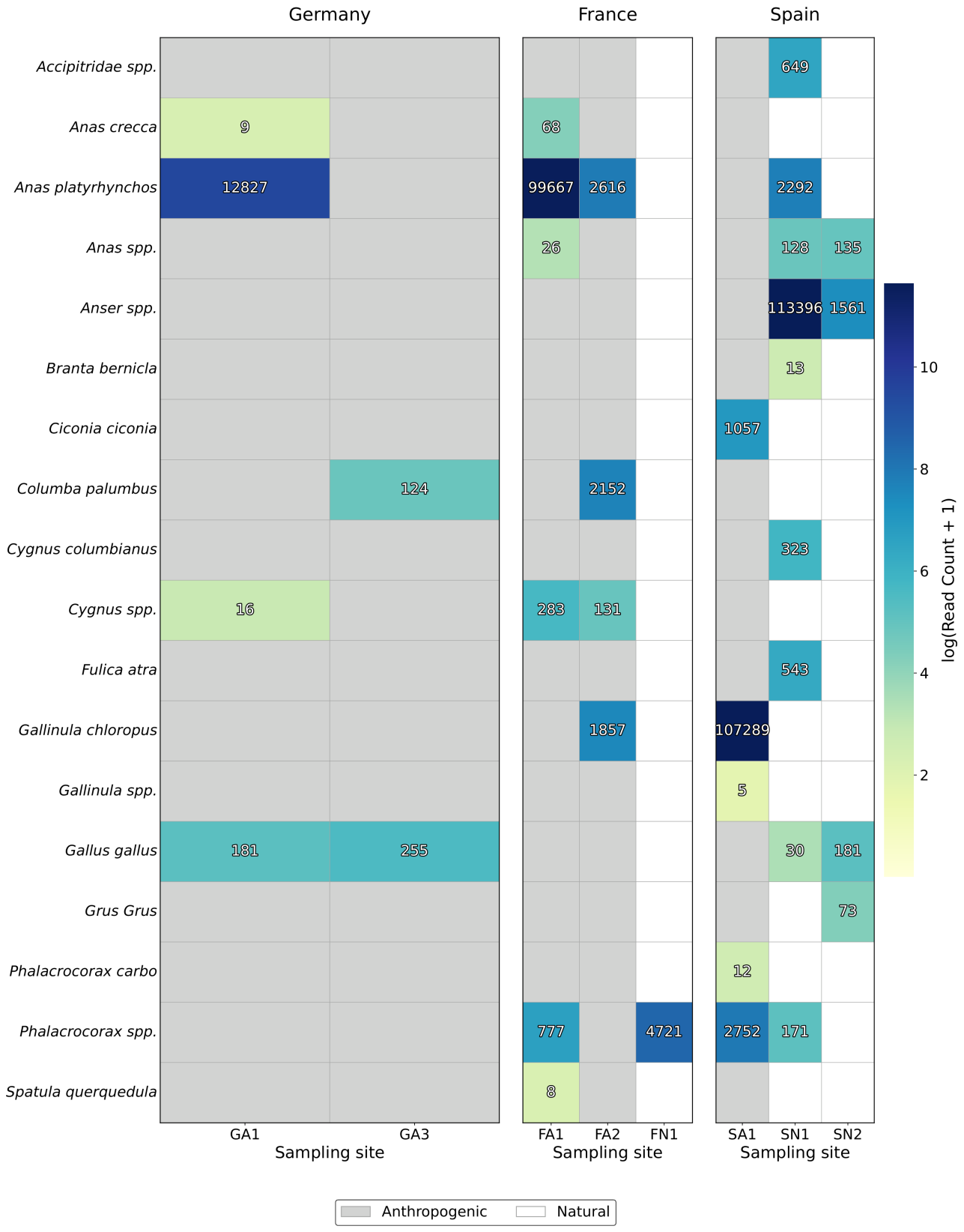

FIG 3 Number of avian species identified from 12S rRNA-based eDNA across wetland sites. Color intensity corresponds to log(read count + 1) aggregated per species and site. Species assignments were restricted to avian species at an identity percentage to the reference of ≥98% and a read count of ≥5. The gray background highlights anthropogenically impacted sites.

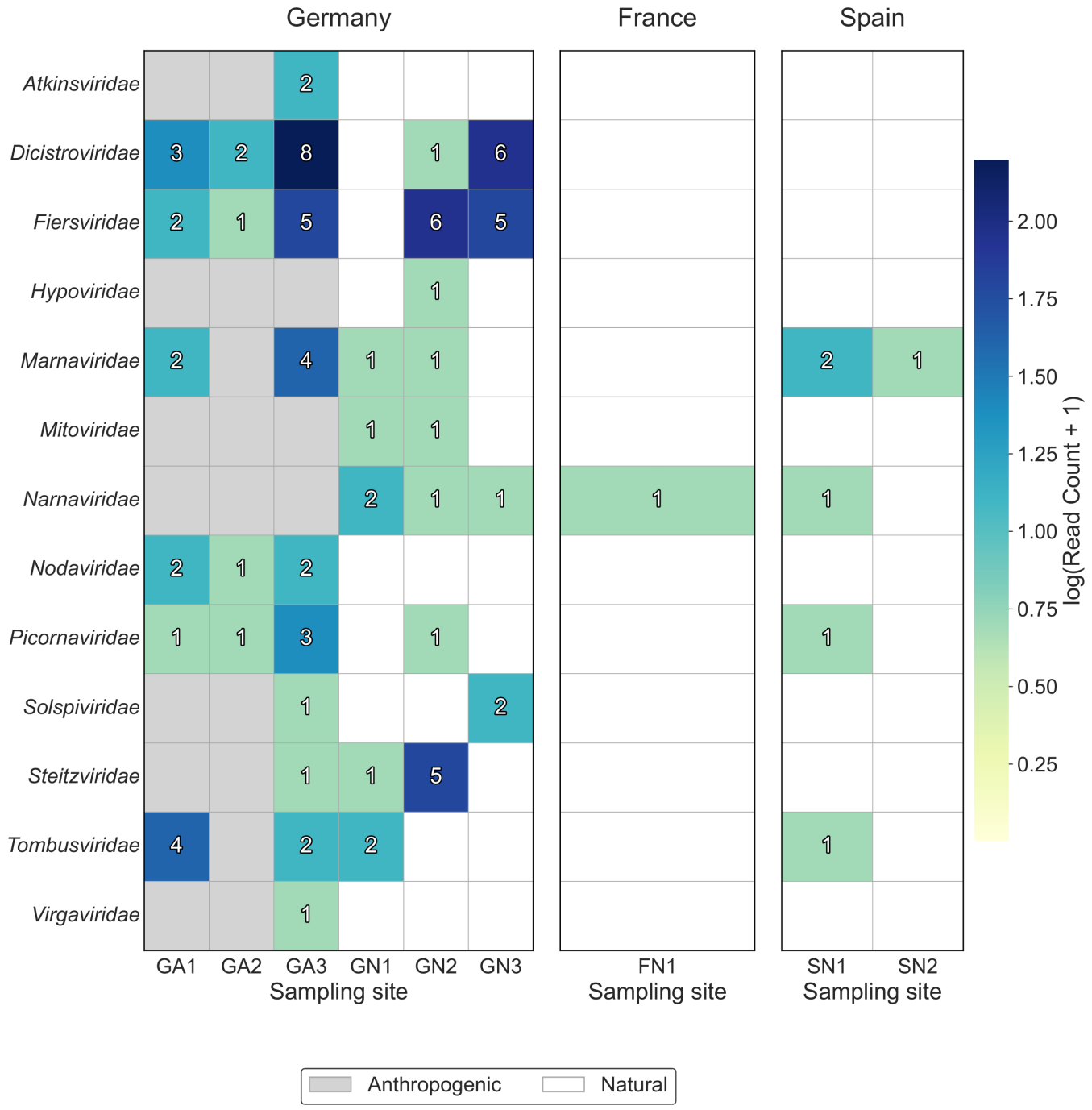

FIG 4 Number of viral family detections from *de novo* assemblies across wetland sites. Color intensity encodes log(contig count + 1) (Materials and Methods). The gray background highlights anthropogenically impacted sites.

cases in wild birds (76). This revealed that AIV detections coincided with the detection of several potential host species (Table 4); for example, at wetland sites adjacent to duck farms (FA1, FA2), AIV detection coincided with the detection of multiple dabbling duck species (*Anas platyrhynchos, Anas crecca,* and *Spatula querquedula*), which are known AIV reservoirs, as well as *Cygnus* spp. (swan) and *Phalacrocorax* spp. (cormorant) species (Table 4). At FA2, where AIV subtyping confirmed an H4 LPAIV, vertebrate eDNA also detected the presence of *Gallinula chloropus* (moorhen) and *Columba palumbus* (wood pigeon) (Table 4).

TABLE 4 Detection and sequencing of AIV across wetland sites[a]

Site	Positive/total replicates	Ct	HA subtype	Potential avian host
FN1	1/6	37	NA	*Phalacrocorax* spp.
FA1	4/5	34, 36, 37, 40	NA	*Anas platyrhynchos* (mallard), *Anas crecca* (teal), *Spatula querquedula* (garganey), *Cygnus* spp. (swans), *Phalacrocorax* spp. (cormorants)
FA2	2/3	37, 38	H4	*Anas platyrhynchos* (mallard), *Gallinula chloropus* (moorhen), *Columba palumbus* (wood pigeon), *Cygnus* spp. (swans)
SN2	1/3	39	NA	*Gallus gallus* (chicken), *Anser* spp. (geese), *Grus grus* (cranes)

[a]Positive detections were confirmed by RT-qPCR (Ct values shown). HA subtyping was performed where possible by multi-segment PCR and whole-genome sequencing. Potential avian hosts were inferred by combining results from vertebrate eDNA analyses by 12S rRNA metabarcoding with official reports of AIV in wild birds. NA, not applicable.

DISCUSSION

Wetlands along the East Atlantic Flyway, environments where human, animal, and ecosystem health are directly linked, are typical One Health interfaces. The close contact between wild birds, domestic animals, and human populations is known to facilitate the circulation of pathogens and antimicrobial resistance across countries (77, 78). Protecting and monitoring these ecosystems is therefore essential not only for biodiversity conservation but also for early warning of transboundary health threats at the wildlife–livestock–human interface. We here present a holistic, accessible, and cost-efficient framework to characterize the pathogen and resistance load of water sources together with their potential associated hosts by combining passive water sampling with nanopore sequencing. We applied this framework to characterize anthropogenically influenced and spatially matched more natural wetland ecosystems along the East Atlantic Flyway, with *de novo* assemblies confirming their presence and enabling direct links between AMR genes and specific pathogens. RNA virome analysis revealed diverse viral families and highlighted both the potential and the current limitations of untargeted viral metagenomics, as highlighted by our subsequent targeted detection and sequencing of AIV, which was not identified by the RNA virome analyses. Finally, eDNA metabarcoding provided inference of potential AIV hosts, offering potentially valuable insights into the wildlife–livestock interface.

The microbial community could be robustly assessed across different wetland sites from metagenomic data obtained from the deployed torpedo-shaped passive sampling devices: the high similarity of the microbial composition at the taxonomic genus level between biological replicates demonstrates the site-specific replicability—similar to what we have previously observed from metagenomics from active air samples (35). Our comparison of microbial *de novo* assembly tools revealed that while the established metaFlye tool yielded more contiguous assemblies (52), the novel nanoMDBG assembler (53) captured more biological insights, including more diverse microbial species annotations and improved gene recovery. This might be explained by metaFlye's default filter discarding reads below 1 kb, which comprise over 50% of our data; this highlights the advantage of nanoMDBG when it comes to fragmented environmental DNA (52, 79).

The metagenomic data contained several pathogens on the read- and assembly-level analysis, despite stringent pathogen filtering criteria (80). Anthropogenically impacted wetlands exhibited a >13-fold higher number of pathogen-associated reads (9,346 reads across 17 species) than their more natural counterparts (703 reads across 15 species). *De novo* assemblies confirmed the presence of potentially clinically relevant bacteria such as *Acinetobacter baumannii*, *Pseudomonas aeruginosa*, and *Stenotrophomonas maltophilia*, and members of the Enterobacteriaceae family (*Citrobacter freundii*, *Escherichia coli*, and *Klebsiella pneumoniae*). Additionally, we were able to generate assemblies of the pathogens *Bacillus cereus*, *Vibrio cholerae*, *Aeromonas caviae*, *Aeromonas hydrophila*, *Aeromonas veronii*, *Pseudomonas putida*, *Mycobacterium intracellulare*, and the fungus *Fusarium oxysporum* (Table S4). The assemblies confirmed that anthropogenically impacted wetland sites harbored more pathogens and in higher relative abundance than natural sites. This might suggest an increased public health risk associated

with anthropogenically impacted wetland sites (81). Among the detected pathogens, *Aeromonas veronii* and *Vibrio cholerae* were most prominent and might be a concern for public health (82–84): at a wetland adjacent to a duck farm, we found high relative abundances of *A. veronii*, an opportunistic pathogen that can cause septicemia in waterfowl and infections in immunocompromised individuals (85, 86). Similarly, *V. cholerae* emerged as a most prominent pathogen at a wetland site in Spain in proximity to a wastewater treatment plant; here, the high relative abundance might be explained by warm, nutrient-rich conditions (87).

We additionally identified the presence of several AMR genes, including clinically relevant ones. Among the 19 detected AMR genes, β-lactamases were the most abundant ones and were mostly detected at the wetland site close to duck farms in France. This site was enriched for bla_{OXA}, $bla_{\text{OXA-956}}$, and bla_{FOX}, and also harbored the carbapenemases *cphA* and *cphA1*. The relatively long nanopore sequencing reads (in our metagenomic data set: median read length of 900 bases) further have the advantage of providing genomic context around the AMR gene from the same physical DNA fragment. This context can be leveraged to assign the gene to its microbial host and therefore assess the potential health consequences of the detected AMR factor. We found that the pathogenic *A. veronii* carried several β-lactamase genes, including bla_{OXA} and *cphA* with known public health relevance (88, 89) and which are consistent with known *Aeromonas*-associated β-lactamase repertoires (89–91). In cases where the taxonomic resolution does not allow for species-level assignments, additional information can be leveraged to better understand the potential impact of detected AMR genes. For example, we detected the $bla_{\text{VCC-1}}$ and bla_{VCC} genes on sequencing reads assigned to the *Vibrio* genus in the same freshwater samples where other reads pointed to a dominance of pathogenic *V. cholerae*, which might suggest the presence of resistant pathogens at these sites (92). *V. cholerae* is one of the few *Vibrio* species capable of persisting in freshwater environments (93, 94). As the sampled sites were freshwater wetlands (i.e., non-marine systems), this ecological trait might facilitate its environmental persistence in these habitats. We further confirmed all the described pathogen-resistance associations based on *de novo* assemblies, which provide more robust evidence than individual reads. Read-based analyses, however, detected more AMR genes than assemblies (210 versus 33 genes)—which could be false-positive hits, or they could be a consequence of assembly-based approaches suffering from imperfect retention of AMR genes compared to read-based analysis (33). We, however, also found additional resistance genes on the assembly level, namely *nreB* on *Acinetobacter pitii*, and *arsB* and *arsC* on *Acidiphilium multivorum*. The presence of the arsenic resistance genes *arsB* and *arsC* in freshwater sources close to duck farms is interesting since arsenic-based compounds were historically used in agriculture, including as growth-promoting additives in poultry and swine feed (95, 96). The additional detection of these genes on the assembly level could be explained by the increased sequence identity of the AMR genes on the contig level (*nreB*: 91.2%; *arsB*: 90.1%; *arsC* [mean]: 94.3%) in comparison to the read level (*nreB*: 86.6%; *arsB*: 86.7%; *arsC* [mean]: 83.0%) where the identities closely missed the default identity threshold by the resistance gene annotation tool (62). While this shows that assemblies can improve the accuracy of certain genomic regions, such *de novo* assemblies have to be understood as computational constructs that fuse sequencing data from different microbial cells. When it comes to pathogen associations of AMR genes, read-based resistance detection should therefore remain the standard.

We further performed random amplification and rapid transposase-based nanopore sequencing (Rapid SMART-9N) to assess the RNA virome captured by the passive samplers. A diverse group of viral families was detected, with the *Picornaviridae* family as the only one with known mammalian and avian hosts. Picornaviruses are non-enveloped viruses that are environmentally stable and often indicate fecal contamination in surface waters (97). Here, *Picornaviridae* were found at all anthropogenically impacted wetland sites where viral contigs were obtained, in contrast to natural sites where they were found in only two out of the six locations. We also detected the *Dicistroviridae*

family, which includes many insect-infecting viruses such as bee-associated viruses with relevance for pollinator health (98). Several contigs were assigned to the *Nodaviridae* family, which includes fish pathogens (betanodaviruses) associated with viral nervous necrosis in marine and freshwater species (99), and to plant-infecting families such as *Tombusviridae* and *Virgaviridae* (100, 101). The remaining families were mostly bacteriophages or mycoviruses, which are expected in these environmental samples (102).

We were not able to reliably classify many viral sequences to species level. More than half of the viral sequences remained completely unclassified, likely reflecting viral dark matter with high levels of unknown viruses (103). This taxonomic resolution could potentially be improved in the future by increasing viral coverage, which could also help with the detection of new viral species through approaches such as phylogenetic placement analysis to resolve divergent lineages (104–106). To achieve higher viral coverage, sequencing depth could be increased, or ribosomal RNA could be depleted; however, both approaches remain cost-prohibitive at the time of this study.

The AIV-comprising viral family *Orthomyxoviridae* was not detected at any site, probably because AIV concentrations were below the limit of detection of our random-amplification method. As AIV is, however, a pathogen of increasing global significance which is known to be transmitted along major migratory routes through avian hosts (107), we additionally applied a targeted approach by qPCR to detect and characterize AIV strains. We found that the torpedo-shaped passive samplers successfully concentrated sufficient environmental viral RNA from water samples to enable AIV detection by qPCR at a third of our sampled wetland sites. We therefore confirmed these samplers as a cost-effective and easy-to-implement tool for avian influenza detection, as previously shown by (25). The majority of our AIV detections were from wetland sites in the area of Toulouse, France, and in close proximity to high concentrations of intensive duck farming for foie gras production. One of the duck farms in whose proximity we sampled suffered from highly pathogenic AIV (HPAIV) outbreaks in 2022 (108), and we have previously detected recurrent LPAIV cases in that region (data not shown). The close proximity of AIV-carrying migratory bird and their wetland habitats to poultry farming is a known concern for public health, with genetically depauperate domesticated birds contributing to the spread and mutations of pathogens in general (10) and to the emergence of HPAIV specifically (12). Our preliminary findings, together with this potential public health risk, might therefore warrant temporally and spatially larger-scale wetland monitoring endeavors using labor- and cost-efficient passive water sampling approaches.

We were only able to subtype one of the detected AIVs by amplification using universal primers and subsequent nanopore sequencing (46), probably due to the low viral quantity and high RNA fragmentation in the water samples (109, 110). This approach could potentially be optimized to obtain whole-genome data of detected AIV in a more robust manner, for example, by using more specific primers to avoid untargeted amplification (111), applying a multiplex PCR targeting several regions of the HA segment to increase sensitivity (112), or using hybridization probe capture for targeted enrichment (109).

We next leveraged the same DNA that we extracted for metagenomic analyses to sequence eDNA for potential avian host detection. Using 12S rRNA amplicons and the capability of nanopore sequencing technology to also profile short reads of less than 100 bp at high sequencing accuracy (40, 41), we detected the presence of several bird species. For example, we found evidence of the geese genus (*Anser* spp.) in a wetland close to Ciudad Real, Spain, where we also detected AIV, and where we have additionally recently detected AIV in geese fecal samples (113). In a wetland adjacent to duck farms in France, we found dominance of duck (*Anas platyrhynchos*) eDNA, and phylogenetic analysis of the recovered AIV HA segment pointed to a H4 viral subtype that was closely related to other H4 subtypes previously detected from *Anas platyrhynchos*. While these results might suggest possible host inferences from non-invasive samples, no direct link can be established given the presence of eDNA of several bird species in most of the samples. In our case, only at one natural wetland site in France, only a single avian

taxon, the cormorant genus (*Phalacrocorax* spp.), was detected alongside AIV and could therefore potentially be inferred as the most likely host. Just such a detection of potential hosts can give valuable information, for example, on what wildlife is at risk of being infected and of serving as pathogen reservoirs and vectors, or which endangered species could be impacted in their recovery. While it has been suggested that shotgun sequencing of environmental samples can detect the presence of vertebrates without any need for targeted amplification (40), we here found that at a standard sequencing depth none of the avian species detected by eDNA were detected by our metagenomic approach, suggesting a need for eDNA approaches for concurrent sensitive host detection.

Our preliminary comparison of anthropogenically impacted and more natural wetland sites is based on a binary land-use classification defined by the presence or absence of direct anthropogenic inputs, rather than on quantitative environmental covariates. Physicochemical parameters such as temperature, salinity, pH, and nutrient concentrations were not measured, which limits our ability to disentangle the specific environmental drivers of the observed differences in pathogen and AMR prevalence. The "natural" classification does not imply the complete absence of anthropogenic pressures, and the observational study design avoids causal attribution of microbiological differences to specific land-use factors. Future studies should integrate geochemical data with microbial and virological profiles to better characterize the environmental determinants of pathogen and resistance gene prevalence in wetland ecosystems.

In conclusion, we demonstrate that passive water sampling followed by nanopore sequencing provides a holistic and cost-efficient approach for real-time surveillance of wetland ecosystems. With a single non-invasive sampling effort, we were able to detect clinically relevant bacterial pathogens and their associated AMR genes, recover an overview of the RNA virome, identify and subtype AIV, and infer potential avian hosts through vertebrate eDNA. In our study of natural and anthropogenically impacted wetland sites across the East Atlantic Flyway, we found that pathogen detection was consistently higher in anthropogenically impacted wetlands, with robust long-read *de novo* assemblies confirming their presence. This integrated approach highlights how passive samplers capture temporally and potentially spatially cumulative signals and, when combined with the versatility of nanopore sequencing, allow for recovering long-read genomic contexts and *de novo* assemblies as well as accurate short-read metabarcodes, with potentially valuable insights into the One Health interface between the environment, wildlife, livestock, and human populations.

ACKNOWLEDGMENTS

We acknowledge the use of LLMs for support in code development. All code was reviewed and verified by the authors.

This study was funded by a German One Health Platform Pilot Project grant awarded to A.P. and L.U. (2824HS010), and a Helmholtz Principal Investigator Grant and the professorship "One Health with focus on microbial genomics and AI" at the University of Zurich Institute for Food Safety and Hygiene awarded to L.U. Sampling and primary processing of samples at Spanish wetlands was cofunded by projects MCIN/AEI/10.13039/501100011033 (grant no. PID2020-114060RR-C32) and PID2023-149441OR-C33 financed by MICIU/AEI /10.13039/501100011033 and for FEDER, EU.

T.R., A.P., and L.U. designed the experiment. T.R. and A.P. conducted the sampling, processing, and data analysis under L.U.'s supervision. T.R., A.P., and L.U. wrote the manuscript. A.S.-C., E.E., K.S., U.H., G.L.L., and J.-L.G. supported the fieldwork; C.-M.M., S.M.-P., and M.R. optimized sampling approaches; G.C. and J.-L.G. helped with viral sample processing; D.-L.G. helped with eDNA analysis. All authors contributed to and approved the manuscript.

AUTHOR AFFILIATIONS

[1]Helmholtz AI, Helmholtz Zentrum München, Neuherberg, Germany

[2]Helmholtz Pioneer Campus, Helmholtz Zentrum München, Neuherberg, Germany
[3]School of Life Sciences, Technical University of Munich, Freising, Germany
[4]Grupo SaBio (Sanidad y Biotecnología), Instituto de Investigación en Recursos Cinegéticos IREC (CSIC-UCLM-JCCM), Ciudad Real, Spain
[5]Laboratory of Viruses Contaminants of Water and Food, Departament de Genètica, Microbiologia i Estadística, Facultat de Biologia, Universitat de Barcelona, Barcelona, Spain
[6]Institut de Recerca de l'Aigua (IdRA), Universitat de Barcelona, Barcelona, Spain
[7]Faunomics, Rifcon GmbH, Goldbeckstraße, Germany
[8]Department of Epidemiology and Ecology of Antimicrobial Resistance, Helmholtz Institute for One Health, Helmholtz Centre for Infection Research HZI, Greifswald, Germany
[9]University Medicine Greifswald, Greifswald, Germany
[10]IHAP, Université de Toulouse, INRAE, ENVT, Toulouse, France
[11]Institute for Food Safety and Hygiene, University of Zurich, Zürich, Switzerland

AUTHOR ORCIDs

Albert Perlas http://orcid.org/0000-0002-4035-2436
Tim Reska http://orcid.org/0009-0001-9700-5128
Cristina Mejías-Molina http://orcid.org/0000-0003-1050-1178
Elias Eger http://orcid.org/0000-0002-5514-8083
Katharina Schaufler http://orcid.org/0000-0002-2669-8799
Ursula Höfle http://orcid.org/0000-0002-6868-079X
Guillaume Le Loc'h http://orcid.org/0000-0001-9621-8474
Lara Urban http://orcid.org/0000-0002-5445-9314

FUNDING

Funder	Grant(s)	Author(s)
German One Health Platform Pilot Project	2824HS010	Albert Perlas Lara Urban
MCIN/AEI/10.13039/501100011033	PID2020-114060RR-C32	Ursula Höfle

DATA AVAILABILITY

All nanopore sequencing raw data have been made available at ENA (PRJEB96272). The AIV H4 obtained consensus sequence was uploaded to GISAID ("A/environment/Occitania/1/2024"; EPI_ISL_20139219). All code has been made publicly available via GitHub: https://github.com/ttmgr/Wetland_Health.

ADDITIONAL FILES

The following material is available online.

Supplemental Material

Supplemental material (AEM02543-25-s0001.docx). Descriptive legends for Tables S1 to S4; Fig. S1 to S4.
Table S1 (AEM02543-25-s0002.xlsx). DNA metagenomics metrics of all samples.
Table S2 (AEM02543-25-s0003.xlsx). RNA virome metrics of all samples.
Table S3 (AEM02543-25-s0004.xlsx). Pathogen species detection of all samples based on sequencing reads.
Table S4 (AEM02543-25-s0005.xlsx). Pathogen species detection of all samples based on nanoMDBG assemblies.

REFERENCES

1. Simpson M, Eldred M, Jayakody S, Mackenzie L, Convention on Wetlands. 2024. Scaling up wetland conservation and restoration to deliver the kunming-montreal global biodiversity framework: guidance on including wetlands in national biodiversity strategy and action plans (NBSAPs) to boost biodiversity and halt wetland loss and degradation. 1st ed. Convention on Wetlands. https://www.ramsar.org/document/scaling-wetland-conservation-restoration-deliver-kunming-montreal-global-biodiversity.
2. Middleton BA. 2017. Climate and land-use change in wetlands: a dedication. Ecosyst Health Sustain 3:1392831. https://doi.org/10.1080/20964129.2017.1392831
3. Fluet-Chouinard E, Stocker BD, Zhang Z, Malhotra A, Melton JR, Poulter B, Kaplan JO, Goldewijk KK, Siebert S, Minayeva T, Hugelius G, Joosten H, Barthelmes A, Prigent C, Aires F, Hoyt AM, Davidson N, Finlayson CM, Lehner B, Jackson RB, McIntyre PB. 2023. Extensive global wetland loss over the past three centuries. Nature 614:281–286. https://doi.org/10.1038/s41586-022-05572-6
4. Horwitz P, Finlayson CM, Weinstein P. 2012. Healthy wetlands, healthy people: a review of wetlands and human health interactions. IWMI Research Reports. https://ideas.repec.org//p/iwt/rerpts/h044745.html.
5. Larsson DGJ, Flach CF. 2022. Antibiotic resistance in the environment. Nat Rev Microbiol 20:257–269. https://doi.org/10.1038/s41579-021-00649-x
6. EClinicalMedicine. 2021. Antimicrobial resistance: a top ten global public health threat. EClinicalMedicine 41:101221. https://doi.org/10.1016/j.eclinm.2021.101221
7. Partridge SR, Kwong SM, Firth N, Jensen SO. 2018. Mobile genetic elements associated with antimicrobial resistance. Clin Microbiol Rev 31:e00088-17. https://doi.org/10.1128/CMR.00088-17
8. Boyd EF, Heilpern AJ, Waldor MK. 2000. Molecular analyses of a putative CTXφ precursor and evidence for independent acquisition of distinct CTXφs by toxigenic *Vibrio cholerae*. J Bacteriol 182:5530–5538. https://doi.org/10.1128/JB.182.19.5530-5538.2000
9. Woolhouse M, Scott F, Hudson Z, Howey R, Chase-Topping M. 2012. Human viruses: discovery and emergence. Phil Trans R Soc B 367:2864–2871. https://doi.org/10.1098/rstb.2011.0354
10. Van Oosterhout C. 2021. Mitigating the threat of emerging infectious diseases; a coevolutionary perspective. Virulence 12:1288–1295. https://doi.org/10.1080/21505594.2021.1920741
11. Hess JC, Paré JA. 2004. Viruses of waterfowl. Semin Avian Exot Pet Med 13:176–183. https://doi.org/10.1053/j.saep.2004.04.002
12. Swayne DE, Suarez DL, Sims LD. 2020. Influenza, p 210–256. *In* Diseases of poultry. John Wiley & Sons, Ltd.
13. Verhagen JH, Fouchier RAM, Lewis N. 2021. Highly pathogenic avian influenza viruses at the wild-domestic bird interface in Europe: future directions for research and surveillance. Viruses 13:212. https://doi.org/10.3390/v13020212
14. Adlhoch C, Fusaro A, Gonzales JL, Kuiken T, Mirinavičiūtė G, Niqueux É, Ståhl K, Staubach C, Terregino C, Willgert K, Baldinelli F, Chuzhakina K, Delacourt R, Georganas A, Georgiev M, Kohnle L, European Food Safety Authority, European Centre for Disease Prevention and Control, European Union Reference Laboratory for Avian Influenza. 2023. Avian influenza overview September-December 2023. EFSA J 21:e8539. https://doi.org/10.2903/j.efsa.2023.8539
15. Caliendo V, Kleyheeg E, Beerens N, Camphuysen KCJ, Cazemier R, Elbers ARW, Fouchier RAM, Kelder L, Kuiken T, Leopold M, Slaterus R, Spierenburg MAH, van der Jeugd H, Verdaat H, Rijks JM. 2024. Effect of 2020–21 and 2021–22 highly pathogenic avian influenza H5 epidemics on wild birds, the Netherlands. Emerg Infect Dis 30:50–57. https://doi.org/10.3201/eid3001.230970
16. Ramey AM, Hill NJ, DeLiberto TJ, Gibbs SEJ, Camille Hopkins M, Lang AS, Poulson RL, Prosser DJ, Sleeman JM, Stallknecht DE, Wan X. 2022. Highly pathogenic avian influenza is an emerging disease threat to wild birds in North America. J Wildl Manag 86:e22171. https://doi.org/10.1002/jwmg.22171
17. Ahrens AK, Selinka H-C, Wylezich C, Wonnemann H, Sindt O, Hellmer HH, Pfaff F, Höper D, Mettenleiter TC, Beer M, Harder TC. 2023. Investigating environmental matrices for use in avian influenza virus surveillance-surface water, sediments, and avian fecal samples. Microbiol Spectr 11:e0266422. https://doi.org/10.1128/spectrum.02664-22
18. Hozalski RM, Zhao X, Kim T, LaPara TM. 2024. On-site filtration of large sample volumes improves the detection of opportunistic pathogens in drinking water distribution systems. Appl Environ Microbiol 90:e0165823. https://doi.org/10.1128/aem.01658-23
19. Deboosere N, Horm SV, Pinon A, Gachet J, Coldefy C, Buchy P, Vialette M. 2011. Development and validation of a concentration method for the detection of influenza a viruses from large volumes of surface water. Appl Environ Microbiol 77:3802–3808. https://doi.org/10.1128/AEM.02484-10
20. Schang C, Crosbie ND, Nolan M, Poon R, Wang M, Jex A, John N, Baker L, Scales P, Schmidt J, Thorley BR, Hill K, Zamyadi A, Tseng C-W, Henry R, Kolotelo P, Langeveld J, Schilperoort R, Shi B, Einsiedel S, Thomas M, Black J, Wilson S, McCarthy DT. 2021. Passive sampling of SARS-CoV-2 for wastewater surveillance. Environ Sci Technol 55:10432–10441. https://doi.org/10.1021/acs.est.1c01530
21. Geissler M, Mayer R, Helm B, Dumke R. 2024. Food and environmental virology: use of passive sampling to characterize the presence of SARS-CoV-2 and other viruses in wastewater. Food Environ Virol 16:25–37. https://doi.org/10.1007/s12560-023-09572-1
22. Habtewold J, McCarthy D, McBean E, Law I, Goodridge L, Habash M, Murphy HM. 2022. Passive sampling, a practical method for wastewater-based surveillance of SARS-CoV-2. Environ Res 204:112058. https://doi.org/10.1016/j.envres.2021.112058
23. Mejías-Molina C, Pico-Tomàs A, Beltran-Rubinat A, Martínez-Puchol S, Corominas L, Rusiñol M, Bofill-Mas S. 2023. Effectiveness of passive sampling for the detection and genetic characterization of human viruses in wastewater. Environ Sci: Water Res Technol 9:1195–1204. https://doi.org/10.1039/D2EW00867J
24. Mejías-Molina C, Estarlich-Landajo I, Martínez-Puchol S, Bofill-Mas S, Rusiñol M. 2024. Exploring waterborne viruses in groundwater: quantification and virome characterization via passive sampling and targeted enrichment sequencing. Water Res 266:122305. https://doi.org/10.1016/j.watres.2024.122305
25. Panzarin V, Crimaudo M, Bonfante F, Marciano S, Berto P, Bofill-Mas S, Rusiñol M, Mazzetto E, Bortolami A, Fornasiero D, Martelli L, Mulatti P, Terregino C. 2025. Exploring the use of passive samplers for the surveillance of avian influenza viruses in wetlands: a laboratory and field validation study. Food Environ Virol 17:37. https://doi.org/10.1007/s12560-025-09649-z
26. McConn BR, Kraft AL, Durso LM, Ibekwe AM, Frye JG, Wells JE, Tobey EM, Ritchie S, Williams CF, Cook KL, Sharma M. 2024. An analysis of culture-based methods used for the detection and isolation of *Salmonella* spp., *Escherichia coli*, and *Enterococcus* spp. from surface water: a systematic review. Sci Total Environ 927:172190. https://doi.org/10.1016/j.scitotenv.2024.172190
27. Pinar-Méndez A, Galofré B, Blanch AR, García-Aljaro C. 2022. Culture and molecular methods as complementary tools for water quality management. Sci Total Environ 848:157789. https://doi.org/10.1016/j.scitotenv.2022.157789
28. Alcolea-Medina A, Alder C, Snell LB, Charalampous T, Aydin A, Nebbia G, Williams T, Goldenberg S, Douthwaite S, Batra R, Cliff PR, Mischo H, Neil S, Wilks M, Edgeworth JD. 2024. Unified metagenomic method for rapid detection of microorganisms in clinical samples. Commun Med (Lond) 4:135. https://doi.org/10.1038/s43856-024-00554-3
29. Claro IM, Ramundo MS, Coletti TM, da Silva CAM, Valenca IN, Candido DS, Sales FCS, Manuli ER, de Jesus JG, de Paula A, Felix AC, Andrade PDS, Pinho MC, Souza WM, Amorim MR, Proenca-Modena JL, Kallas EG, Levi JE, Faria NR, Sabino EC, Loman NJ, Quick J. 2021. Rapid viral metagenomics using SMART-9N amplification and nanopore sequencing. Wellcome Open Res 6:241. https://doi.org/10.12688/wellcomeopenres.17170.2
30. Oxford Nanopore Technologies. 2023. Rapid metagenomic sequencing for surveillance of bacterial, fungal and viral pathogens using SQK-RPB114.24. Available from: https://nanoporetech.com/document/rapid-sequencing-metagenomics-sqk-rpb114-24
31. Chen L, Zhao N, Cao J, Liu X, Xu J, Ma Y, Yu Y, Zhang X, Zhang W, Guan X, Yu X, Liu Z, Fan Y, Wang Y, Liang F, Wang D, Zhao L, Song M, Wang J. 2022. Short- and long-read metagenomics expand individualized structural variations in gut microbiomes. Nat Commun 13:3175. https://doi.org/10.1038/s41467-022-30857-9
32. Che Y, Xia Y, Liu L, Li AD, Yang Y, Zhang T. 2019. Mobile antibiotic resistome in wastewater treatment plants revealed by Nanopore

metagenomic sequencing. Microbiome 7:44. https://doi.org/10.1186/s40168-019-0663-0
33. Cottingham H, Judd LM, Harshegyi-Hand T, Wisniewski JA, Blakeway LV, Hong T, Parker MH, Peleg AY, Holt KE, Hawkey J, Macesic N. 2025. Nanopore sequencing enables highly accurate genotyping and identification of resistance determinants in key nosocomial pathogens. medRxiv. https://doi.org/10.1101/2025.07.24.25332173
34. Dai D, Brown C, Bürgmann H, Larsson DGJ, Nambi I, Zhang T, Flach C-F, Pruden A, Vikesland PJ. 2022. Long-read metagenomic sequencing reveals shifts in associations of antibiotic resistance genes with mobile genetic elements from sewage to activated sludge. Microbiome 10:20. https://doi.org/10.1186/s40168-021-01216-5
35. Reska T, Pozdniakova S, Borràs S, Perlas A, Sauerborn E, Cañas L, Schloter M, Rodó X, Wang Y, Winkler B, Schnitzler J-P, Urban L. 2024. Air monitoring by nanopore sequencing. ISME Commun 4:ycae099. https://doi.org/10.1093/ismeco/ycae099
36. Urban L, Perlas A, Francino O, Martí-Carreras J, Muga BA, Mwangi JW, Boykin Okalebo L, Stanton J-AL, Black A, Waipara N, Fontsere C, Eccles D, Urel H, Reska T, Morales HE, Palmada-Flores M, Marques-Bonet T, Watsa M, Libke Z, Erkenswick G, van Oosterhout C. 2023. Real-time genomics for One Health. Mol Syst Biol 19:e11686. https://doi.org/10.15252/msb.202311686
37. Chang WS, Eden JS, Hall J, Shi M, Rose K, Holmes EC. 2020. Metatranscriptomic analysis of virus diversity in urban wild birds with paretic disease. J Virol 94:e00606-20. https://doi.org/10.1128/JVI.00606-20
38. Mirza JD, de Oliveira Guimarães L, Wilkinson S, Rocha EC, Bertanhe M, Helfstein VC, de-Deus JT, Claro IM, Cumley N, Quick J, Faria NR, Sabino EC, Kirchgatter K, Loman NJ. 2024. Tracking arboviruses, their transmission vectors and potential hosts by nanopore sequencing of mosquitoes. Microb Genom 10:001184. https://doi.org/10.1099/mgen.0.001184
39. Moreno KMF, de Andrade VA, de Melo Iani FC, Fonseca V, Lima MT, de Castro Barbosa E, Tomé LMR, Guimarães NR, Fritsch HM, Adelino T, Oliveira Fereguetti T, Aspahan MC, Gamarano Barros T, Alcantara LCJ, Giovanetti M. 2024. Exploring microorganisms associated to acute febrile illness and severe neurological disorders of unknown origin: a nanopore metagenomics approach. Genes (Basel) 15:922. https://doi.org/10.3390/genes15070922
40. Bista I, Lino A. 2025. Long-read sequencing for biodiversity analyses - a comprehensive guide. Biodiversity. https://doi.org/10.32942/X2JP8H
41. Gygax D, Ramirez S, Chibesa M, Simpamba T, Riffel M, Riffel T, Zulu G, Srivathsan A, Nijland R, Urban L. 2025. Evaluation of nanopore sequencing for increasing accessibility of eDNA studies in biodiverse countries. bioRxiv. https://doi.org/10.1101/2025.04.21.649756
42. Riaz T, Shehzad W, Viari A, Pompanon F, Taberlet P, Coissac E. 2011. ecoPrimers: inference of new DNA barcode markers from whole genome sequence analysis. Nucleic Acids Res 39:e145. https://doi.org/10.1093/nar/gkr732
43. Calvignac-Spencer S, Merkel K, Kutzner N, Kühl H, Boesch C, Kappeler PM, Metzger S, Schubert G, Leendertz FH. 2013. Carrion fly-derived DNA as a tool for comprehensive and cost-effective assessment of mammalian biodiversity. Mol Ecol 22:915–924. https://doi.org/10.1111/mec.12183
44. Heine HG, Trinidad L, Selleck P, Lowther S. 2007. Rapid detection of highly pathogenic avian influenza H5N1 virus by TaQman reverse transcriptase–polymerase chain reaction. Avian Dis 51:370–372. https://doi.org/10.1637/7587-040206R.1
45. Bessière P, Hayes B, Filaire F, Lèbre L, Vergne T, Pinson M, Croville G, Guérin J-L. 2023. Optimizing environmental viral surveillance: bovine serum albumin increases RT-qPCR sensitivity for high pathogenicity avian influenza H5Nx virus detection from dust samples. Microbiol Spectr 11:e0305523. https://doi.org/10.1128/spectrum.03055-23
46. Perlas A, Reska T, Croville G, Tarrés-Freixas F, Guérin J-L, Majó N, Urban L. 2025. Improvements in RNA and DNA nanopore sequencing allow for rapid genetic characterization of avian influenza. Virus Evol 11:veaf010. https://doi.org/10.1093/ve/veaf010
47. GitHub. 2025. Nanoporetech/dorado: Oxford Nanopore's Basecaller. Available from: https://github.com/nanoporetech/dorado
48. Wick R. 2025. Rrwick/Porechop [C++]. Available from: https://github.com/rrwick/Porechop
49. De Coster W, D'Hert S, Schultz DT, Cruts M, Van Broeckhoven C. 2018. NanoPack: visualizing and processing long-read sequencing data. Bioinformatics 34:2666–2669. https://doi.org/10.1093/bioinformatics/bty149
50. Wood DE, Lu J, Langmead B. 2019. Improved metagenomic analysis with Kraken 2. Genome Biol 20:257. https://doi.org/10.1186/s13059-019-1891-0
51. Shen W, Le S, Li Y, Hu F. 2016. SeqKit: a cross-platform and ultrafast toolkit for FASTA/Q file manipulation. PLoS One 11:e0163962. https://doi.org/10.1371/journal.pone.0163962
52. Kolmogorov M, Bickhart DM, Behsaz B, Gurevich A, Rayko M, Shin SB, Kuhn K, Yuan J, Polevikov E, Smith TPL, Pevzner PA. 2020. metaFlye: scalable long-read metagenome assembly using repeat graphs. Nat Methods 17:1103–1110. https://doi.org/10.1038/s41592-020-00971-x
53. Benoit G, James R, Raguideau S, Alabone G, Goodall T, Chikhi R, Quince C. 2025 High-quality metagenome assembly from nanopore reads with nanoMDBG. Bioinformatics. https://doi.org/10.1101/2025.04.22.649928
54. Li H. 2018. Minimap2: pairwise alignment for nucleotide sequences. Bioinformatics 34:3094–3100. https://doi.org/10.1093/bioinformatics/bty191
55. Vaser R, Sović I, Nagarajan N, Šikić M. 2017. Fast and accurate de novo genome assembly from long uncorrected reads. Genome Res 27:737–746. https://doi.org/10.1101/gr.214270.116
56. Wright C. 2025. Nanoporetech/medaka. Oxford Nanopore Technologies. Available from: https://github.com/nanoporetech/medaka
57. Seemann T. 2014. Prokka: rapid prokaryotic genome annotation. Bioinformatics 30:2068–2069. https://doi.org/10.1093/bioinformatics/btu153
58. Huson DH, Beier S, Flade I, Górska A, El-Hadidi M, Mitra S, Ruscheweyh H-J, Tappu R. 2016. MEGAN community edition - interactive exploration and analysis of large-scale microbiome sequencing data. PLoS Comput Biol 12:e1004957. https://doi.org/10.1371/journal.pcbi.1004957
59. Chan Zuckerberg ID. 2025. The free, cloud-based metagenomics platform. Available from: https://czid.org/pathogen_list v0.2.1
60. Chen L, Yang J, Yu J, Yao Z, Sun L, Shen Y. 2004. VFDB: a reference database for bacterial virulence factors. Nucleic Acids Res 33:D325–D328. https://doi.org/10.1093/nar/gki008
61. Buchfink B, Xie C, Huson DH. 2015. Fast and sensitive protein alignment using DIAMOND. Nat Methods 12:59–60. https://doi.org/10.1038/nmeth.3176
62. Feldgarden M, Brover V, Gonzalez-Escalona N, Frye JG, Haendiges J, Haft DH, Hoffmann M, Pettengill JB, Prasad AB, Tillman GE, Tyson GH, Klimke W. 2021. AMRFinderPlus and the Reference Gene Catalog facilitate examination of the genomic links among antimicrobial resistance, stress response, and virulence. Sci Rep 11:12728. https://doi.org/10.1038/s41598-021-91456-0
63. Hyatt D, Chen G-L, Locascio PF, Land ML, Larimer FW, Hauser LJ. 2010. Prodigal: prokaryotic gene recognition and translation initiation site identification. BMC Bioinformatics 11:119. https://doi.org/10.1186/1471-2105-11-119
64. Carattoli A, Zankari E, García-Fernández A, Voldby Larsen M, Lund O, Villa L, Møller Aarestrup F, Hasman H. 2014. *In silico* detection and typing of plasmids using PlasmidFinder and plasmid multilocus sequence typing. Antimicrob Agents Chemother 58:3895–3903. https://doi.org/10.1128/AAC.02412-14
65. Boyer F, Mercier C, Bonin A, Le Bras Y, Taberlet P, Coissac E. 2016. Obitools: a unix-inspired software package for DNA metabarcoding. Mol Ecol Resour 16:176–182. https://doi.org/10.1111/1755-0998.12428
66. Martin M. 2011. Cutadapt removes adapter sequences from high-throughput sequencing reads. EMBnet j 17:10. https://doi.org/10.14806/ej.17.1.200
67. Rognes T, Flouri T, Nichols B, Quince C, Mahé F. 2016. VSEARCH: a versatile open source tool for metagenomics. PeerJ 4:e2584. https://doi.org/10.7717/peerj.2584
68. Leray M, Knowlton N, Machida RJ. 2022. MIDORI2: a collection of quality controlled, preformatted, and regularly updated reference databases for taxonomic assignment of eukaryotic mitochondrial sequences. Environmental DNA 4:894–907. https://doi.org/10.1002/edn3.303
69. Li H, Handsaker B, Wysoker A, Fennell T, Ruan J, Homer N, Marth G, Abecasis G, Durbin R, 1000 Genome Project Data Processing Subgroup. 2009. The sequence alignment/map format and SAMtools. Bioinformatics 25:2078–2079. https://doi.org/10.1093/bioinformatics/btp352
70. Li H. 2011. A statistical framework for SNP calling, mutation discovery, association mapping and population genetical parameter estimation from sequencing data. Bioinformatics 27:2987–2993. https://doi.org/10.1093/bioinformatics/btr509
71. Khare S, Gurry C, Freitas L, Schultz MB, Bach G, Diallo A, Akite N, Ho J, Lee RT, Yeo W, Curation Team GC, Maurer-Stroh S. 2021. GISAID's role in

pandemic response. China CDC Wkly 3:1049–1051. https://doi.org/10.46234/ccdcw2021.255
72. Katoh K, Standley DM. 2013. MAFFT multiple sequence alignment software version 7: improvements in performance and usability. Mol Biol Evol 30:772–780. https://doi.org/10.1093/molbev/mst010
73. Minh BQ, Schmidt HA, Chernomor O, Schrempf D, Woodhams MD, von Haeseler A, Lanfear R. 2020. IQ-TREE 2: new models and efficient methods for phylogenetic inference in the genomic era. Mol Biol Evol 37:1530–1534. https://doi.org/10.1093/molbev/msaa015
74. Letunic I, Bork P. 2024. Interactive Tree of Life (iTOL) v6: recent updates to the phylogenetic tree display and annotation tool. Nucleic Acids Res 52:W78–W82. https://doi.org/10.1093/nar/gkae268
75. Docquier J-D, Pantanella F, Giuliani F, Thaller MC, Amicosante G, Galleni M, Frère J-M, Bush K, Rossolini GM. 2002. CAU-1, a subclass B3 metallo-β-lactamase of low substrate affinity encoded by an ortholog present in the *Caulobacter crescentus* chromosome. Antimicrob Agents Chemother 46:1823–1830. https://doi.org/10.1128/AAC.46.6.1823-1830.2002
76. Empres-i +. 2025. Rome, Italy. Food and Agriculture Organization of the United Nations (FAO). https://empres-i.apps.fao.org/general.
77. Gass JD Jr, Dusek RJ, Hall JS, Hallgrimsson GT, Halldórsson HP, Vignisson SR, Ragnarsdottir SB, Jónsson JE, Krauss S, Wong S-S, Wan X-F, Akter S, Sreevatsan S, Trovão NS, Nutter FB, Runstadler JA, Hill NJ. 2023. Global dissemination of influenza A virus is driven by wild bird migration through arctic and subarctic zones. Mol Ecol 32:198–213. https://doi.org/10.1111/mec.16738
78. Zeballos-Gross D, Rojas-Sereno Z, Salgado-Caxito M, Poeta P, Torres C, Benavides JA. 2021. The role of gulls as reservoirs of antibiotic resistance in aquatic environments: a scoping review. Front Microbiol 12:703886. https://doi.org/10.3389/fmicb.2021.703886
79. Sahu A, Singh M, Amin A, Malik MM, Qadri SN, Abubakr A, Teja SS, Dar SA, Ahmad I. 2025. A systematic review on environmental DNA (eDNA) acience: an eco-friendly survey method for conservation and restoration of fragile ecosystems. Ecol Indic 173:113441. https://doi.org/10.1016/j.ecolind.2025.113441
80. Nielsen ME, Søgaard KK, Karst SM, Krarup AL, Albertsen M, Nielsen HL. 2025. Application of rapid Nanopore metagenomic cell-free DNA sequencing to diagnose bloodstream infections: a prospective observational study. Microbiol Spectr 13:e0329524. https://doi.org/10.1128/spectrum.03295-24
81. Ballesteros N, Páez L, Luna N, Reina A, Urrea V, Sánchez C, Ramírez A, Ramirez JD, Muñoz M. 2023. Characterization of microbial communities in seven wetlands with different anthropogenic burden using Next Generation Sequencing in Bogotá, Colombia. Sci Rep 13:16973. https://doi.org/10.1038/s41598-023-42970-w
82. Hall CW, Mah TF. 2017. Molecular mechanisms of biofilm-based antibiotic resistance and tolerance in pathogenic bacteria. FEMS Microbiol Rev 41:276–301. https://doi.org/10.1093/femsre/fux010
83. Talagrand-Reboul E, Jumas-Bilak E, Lamy B. 2017. The social life of *Aeromonas* through biofilm and quorum sensing systems. Front Microbiol 8:37. https://doi.org/10.3389/fmicb.2017.00037
84. Yildiz FH, Visick KL. 2009. *Vibrio* biofilms: so much the same yet so different. Trends Microbiol 17:109–118. https://doi.org/10.1016/j.tim.2008.12.004
85. Mencacci A, Cenci E, Mazzolla R, Farinelli S, D'Alò F, Vitali M, Bistoni F. 2003. *Aeromonas veronii* biovar veronii septicaemia and acute suppurative cholangitis in a patient with hepatitis B. J Med Microbiol 52:727–730. https://doi.org/10.1099/jmm.0.05214-0
86. Semwal A, Kumar A, Kumar N. 2023. A review on pathogenicity of *Aeromonas hydrophila* and their mitigation through medicinal herbs in aquaculture. Heliyon 9:e14088. https://doi.org/10.1016/j.heliyon.2023.e14088
87. Wong YY, Lee CW, Bong CW, Lim JH, Ng CC, Narayanan K, Sim EUH, Wang A. 2024. Environmental factors that regulate *Vibrio* spp. abundance and community structure in tropical waters. Anthropocene Coasts 7:21. https://doi.org/10.1007/s44218-024-00054-w
88. Bush K. 2013. Proliferation and significance of clinically relevant β-lactamases. Ann N Y Acad Sci 1277:84–90. https://doi.org/10.1111/nyas.12023
89. Bush K, Bradford PA. 2020. Epidemiology of β-lactamase-producing pathogens. Clin Microbiol Rev 33:e00047-19. https://doi.org/10.1128/CMR.00047-19
90. Piotrowska M, Przygodzińska D, Matyjewicz K, Popowska M. 2017. Occurrence and variety of β-lactamase genes among *Aeromonas* spp. isolated from urban wastewater treatment plant. Front Microbiol 8:863. https://doi.org/10.3389/fmicb.2017.00863
91. Sinclair HA, Heney C, Sidjabat HE, George NM, Bergh H, Anuj SN, Nimmo GR, Paterson DL. 2016. Genotypic and phenotypic identification of *Aeromonas* species and CphA-mediated carbapenem resistance in Queensland, Australia. Diagn Microbiol Infect Dis 85:98–101. https://doi.org/10.1016/j.diagmicrobio.2016.02.005
92. Mangat CS, Boyd D, Janecko N, Martz S-L, Desruisseau A, Carpenter M, Reid-Smith RJ, Mulvey MR. 2016. Characterization of VCC-1, a novel ambler class A carbapenemase from vibrio cholerae isolated from imported retail shrimp sold in Canada. Antimicrob Agents Chemother 60:1819–1825. https://doi.org/10.1128/AAC.02812-15
93. Awere-Duodu A, Ntim OK, Donkor ES. 2025. *Vibrio cholerae* in water environments: a systematic review and meta-analysis. Environ Microbiol Rep 17:e70103. https://doi.org/10.1111/1758-2229.70103
94. Daboul J, Weghorst L, DeAngelis C, Plecha SC, Saul-McBeth J, Matson JS. 2020. Characterization of *Vibrio cholerae* isolates from freshwater sources in northwest Ohio. PLoS One 15:e0238438. https://doi.org/10.1371/journal.pone.0238438
95. Kabiraj A, Biswas R, Halder U, Bandopadhyay R. 2022. Bacterial arsenic metabolism and its role in arsenic bioremediation. Curr Microbiol 79:131. https://doi.org/10.1007/s00284-022-02810-y
96. Upadhyay MK, Shukla A, Yadav P, Srivastava S. 2019. A review of arsenic in crops, vegetables, animals and food products. Food Chem 276:608–618. https://doi.org/10.1016/j.foodchem.2018.10.069
97. Fong TT, Lipp EK. 2005. Enteric viruses of humans and animals in aquatic environments: health risks, detection, and potential water quality assessment tools. Microbiol Mol Biol Rev 69:357–371. https://doi.org/10.1128/MMBR.69.2.357-371.2005
98. McMenamin AJ, Flenniken ML. 2018. Recently identified bee viruses and their impact on bee pollinators. Curr Opin Insect Sci 26:120–129. https://doi.org/10.1016/j.cois.2018.02.009
99. Pefanis SM, Knowles G, Mohr PG, Swift K, Bergfeld J, Wilson TK, Douglas M, Hawkins R, Hoad J, Costin A, Morris J, Cummins D, Moody NJG. 2025. Viral nervous necrosis due to betanodavirus: a case study in pot-bellied seahorses (*Hippocampus abdominals*). J Fish Dis 48:e14131. https://doi.org/10.1111/jfd.14131
100. Santala J, Samuilova O, Hannukkala A, Latvala S, Kortemaa H, Beuch U, Kvarnheden A, Persson P, Topp K, Ørstad K, et al. 2010. Detection, distribution and control of *Potato mop - top virus*, a soil - borne virus, in northern Europe. Ann Appl Biol 157:163–178. https://doi.org/10.1111/j.1744-7348.2010.00423.x
101. Yamamura Y, Scholthof HB. 2005. Tomato bushy stunt virus: a resilient model system to study virus-plant interactions. Mol Plant Pathol 6:491–502. https://doi.org/10.1111/j.1364-3703.2005.00301.x
102. Clokie MRJ, Millard AD, Letarov AV, Heaphy S. 2011. Phages in nature. Bacteriophage 1:31–45. https://doi.org/10.4161/bact.1.1.14942
103. Krishnamurthy SR, Wang D. 2017. Origins and challenges of viral dark matter. Virus Res 239:136–142. https://doi.org/10.1016/j.virusres.2017.02.002
104. Chang W-S, Harvey E, Mahar JE, Firth C, Shi M, Simon-Loriere E, Geoghegan JL, Wille M. 2024. Improving the reporting of metagenomic virome-scale data. Commun Biol 7:1687. https://doi.org/10.1038/s42003-024-07212-3
105. Cobbin JC, Charon J, Harvey E, Holmes EC, Mahar JE. 2021. Current challenges to virus discovery by meta-transcriptomics. Curr Opin Virol 51:48–55. https://doi.org/10.1016/j.coviro.2021.09.007
106. Costa VA, Bellwood DR, Mifsud JCO, Geoghegan JL, Harvey E, Holmes EC. 2025. Limited similarity in microbial composition among coral reef fishes from the Great Barrier Reef, Australia. FEMS Microbiol Ecol 101:fiaf016. https://doi.org/10.1093/femsec/fiaf016
107. Signore AV, Giacinti J, Jones MEB, Erdelyan CNG, McLaughlin A, Alkie TN, Cox S, Lair S, Jardine CM, Stevens B, et al. 2025. Spatiotemporal reconstruction of the North American A(H5N1) outbreak reveals successive lineage replacements by descendant reassortants. Sci Adv 11:eadu4909. https://doi.org/10.1126/sciadv.adu4909
108. Adlhoch C, Fusaro A, Gonzales JL, Kuiken T, Marangon S, Niqueux É, Staubach C, Terregino C, Aznar I, Guajardo IM, Baldinelli F, European Food Safety Authority, European Centre for Disease Prevention and Control, European Union Reference Laboratory for Avian Influenza. 2022. Avian influenza overview March – June 2022. EFS2 20:e07415. https://doi.org/10.2903/j.efsa.2022.7415
109. Kuchinski KS, Coombe M, Mansour SC, Cortez GAP, Kalhor M, Himsworth CG, Prystajecky NA. 2024. Targeted genomic sequencing of

avian influenza viruses in wetland sediment from wild bird habitats. Appl Environ Microbiol 90:e0084223. https://doi.org/10.1128/aem.00842-23
110. Tindale LC, Baticados W, Duan J, Coombe M, Jassem A, Tang P, Uyaguari-Diaz M, Moore R, Himsworth C, Hsiao W, Prystajecky N. 2020. Extraction and detection of avian influenza virus from wetland sediment using enrichment-based targeted resequencing. Front Vet Sci 7:301. https://doi.org/10.3389/fvets.2020.00301
111. Goraichuk IV, Risalvato J, Pantin-Jackwood M, Suarez DL. 2024. Improved influenza A whole-genome sequencing protocol. Front Cell Infect Microbiol 14:1497278. https://doi.org/10.3389/fcimb.2024.1497278
112. Croville G, Walch M, Sécula A, Lèbre L, Silva S, Filaire F, Guérin J-L. 2024. An amplicon-based nanopore sequencing workflow for rapid tracking of avian influenza outbreaks, France, 2020-2022. Front Cell Infect Microbiol 14:1257586. https://doi.org/10.3389/fcimb.2024.1257586
113. Bárbara A, Torrontegi O, Camacho MC, Barral M, Hernández JM, Höfle U. 2017. Avian influenza virus surveillance in south-central Spain using fecal samples of aquatic birds foraging at landfills. Front Vet Sci 4:178. https://doi.org/10.3389/fvets.2017.00178